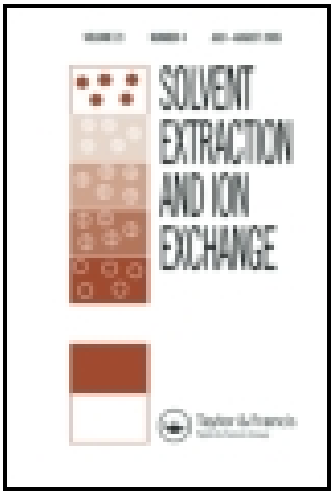


Solvent Extraction and Ion Exchange
Publication details, including instructions for authors and subscription information:
http://www.tandfonline.com/loi/lsei20

# REAGENT-FREE ION-EXCHANGE SEPARATIONS

Vladimir I. Gorshkov [a] & Vladimir A. Ivanov [a]
[a] Department of Physical Chemistry , Chemical Faculty, Lomonosov Moscow State University , Moscow, 119899, Russia
Published online: 10 May 2007.

To cite this article: Vladimir I. Gorshkov & Vladimir A. Ivanov (1999) REAGENT-FREE ION-EXCHANGE SEPARATIONS, Solvent Extraction and Ion Exchange, 17:4, 695-766, DOI: 10.1080/07366299908934634

To link to this article: http://dx.doi.org/10.1080/07366299908934634

SOLVENT EXTRACTION AND ION EXCHANGE, 17(4), 695–766 (1999)

# REAGENT-FREE ION-EXCHANGE SEPARATIONS

Vladimir I. Gorshkov and Vladimir A. Ivanov

Department of Physical Chemistry, Chemical Faculty, Lomonosov Moscow State University, 119899 Moscow, Russia.



## ABSTRACT

This paper reviews the development of reagent-free (and therefore ecologically clean) ion-exchange separation techniques. These methods are based on the shift of the ion exchanger selectivity induced by the modulation of some physico-chemical parameters of the system such as temperature, solution concentration, pH, etc. This approach avoids the use of auxiliary reagents and additional operations such as the regeneration of ion-exchange resin and auxiliary chemicals for their reuse. It also minimizes the amount of toxic wastes produced.

## LIST OF CONTENTS

## 1. INTRODUCTION

Most conventional ion-exchange separation methods are based on application of auxiliary reagents, which are mainly used for displacing the ion mixture being separated from the ion exchanger. The use of auxiliary reagents complicates the process because of the need to include additional operations such as the regeneration of ion exchanger and auxiliary chemicals for their reuse. These additional operations require in turn, additional expenditure of reagents, energy, manpower, etc., and result in increase of wastes produced. Moreover, in certain instances application of auxiliary reagents can lead to recontamination of the purified products. These drawbacks can be considered as the main limitation factors hampering the wide application of large-scale ion exchange separation processes.

To avoid the above drawbacks one can use the shift of ion-exchanger selectivity towards mixture components that results from the modulation of some physico-chemical parameters of the system such as temperature, solution concentration, pH, etc. This paper discusses the results obtained on the development of ecologically clean reagent-free ion-exchange methods based upon this concept.



## 1a. Ion-Exchange Selectivity

The selectivity of an ion exchanger towards ions A and B is usually characterized by the magnitude of either equilibrium separation coefficient $\alpha$

$$\alpha = \frac{y_A}{y_B} \Big/ \frac{x_A}{x_B} \tag{1}$$

or selectivity coefficient $K$

$$K = \frac{y_A^{1/z_A}}{y_B^{1/z_B}} \Big/ \frac{x_A^{1/z_A}}{x_B^{1/z_B}} \tag{2}$$

Here $y$ and $x$ are the equivalent fractions of components in the resin and solution phases, respectively; $z_A$ and $z_B$ are the charges of ions; subscripts A and B denoting corresponding ions are usually chosen so that $\alpha > 1$ and $K > 1$.

When one component in the binary mixture is present in great excess, equation (1) can be simplified when, e.g. $x_A \ll 1$ and $y_A \ll 1$ as follows:

$$\alpha = y_A / x_A \tag{1a}$$

In the opposite situation, i.e. when $x_B \ll 1$ and $y_B \ll 1$, equation (1) can be rewritten in the following form:

$$\alpha = x_B / y_B \tag{1b}$$

In the general case both $\alpha$ and $K$ depend on the ratio of exchanging ions in the ion exchanger phase. If the system does not differ dramatically from the ideal one, then at a constant total concentration of equilibrium solution (equiv/l) the $K$ value does not vary significantly with the composition. At the same time for ions with different charges $\alpha$ value varies more significantly. For example, in case of exchange of the divalent ion A and monovalent ion B, $\alpha$ and $K$ values are related as follows:

$$\alpha = K^2 \cdot \frac{y_B}{x_B} \tag{3}$$

Relation (3) shows the variation limits for $\alpha$: which can be defined as follows:

$$\alpha = K^2 \qquad \text{at } y_A \to 0 \text{ and } x_A \to 0 \tag{3a}$$

$$\alpha = K \qquad \text{at } y_A \to 1 \text{ and } x_A \to 1 \tag{3b}$$

In general, the equilibrium dependence $y=f(x)$ (or its reciprocal function $x=g(y)$) can be very complicated.

The selectivity of ion-exchange resins depends on physico-chemical parameters such as temperature, solution concentration, pH, solvent composition and others [1]. The influence of temperature on equilibrium properties of ion-exchange resins (mainly strong acid sulfonate cation exchangers) has been studied by many researchers [2-4]. It is known that the selectivity of resins usually slightly decreases with increasing temperature for equally charged ions exchange, but increases in case of monovalent-divalent cation exchange. As the result, it was generally accepted that

temperature had little influence on equilibrium of most ion exchange systems [1, p.166; 5, Ch.3]. At the same time, a strong influence of temperature on $Ca^{2+}$-$Na^{+}$ [6, 7] and $Mg^{2+}$-$NH_4^{+}$ equilibrium [8] on carboxylic resins was also reported. A significant influence of temperature on sorption of alkali metal chlorides on some polyampholytes has been also found and studied in detail [9-11]. The temperature dependence of cation exchange equilibrium on resins of non-sulfonate types was much less intensively studied until recently, while for some of them a remarkable influence of temperature on selectivity was found [12-14].

The selectivity of ion-exchange resins also depends on the following parameters: 1) total solution concentration [1, Chap. 4, 5] (for exchange of differently charged ions, in particular); 2) pH of solution (for some polyfunctional ion exchangers [17, 18]); 3) presence of complexing agents in solution [1, Chap.2, 5, 6, 15, 19]; 4) solvent composition [19, Chap.3; 20, Chap.1, 2, 3.11], and some others.

The ion-exchange separation methods based on a shift of resin selectivity induced by the change of some physical-chemical parameters of the system were developed during the last three decades. Almost all of the earlier reviews published on this subject [21-23] discussed only the dual-temperature separations using the parametric pumping technique. At the same time some other approaches to reagent-less ion-exchange separation have been successfully developed in Russia since the beginning of 60's [24-28]. The results of these studies (as well as many other studies by Russian scientists in this field) are practically unknown to the researchers beyond Russia working in the same area, e.g. on development of dual-temperature counter-current ion exchange processes [see, e.g. 29-31]. These techniques will be discussed below in comparison with conventional ion-exchange separation methods.

## 2. SINGLE STAGE OPERATION

If the ion exchanger demonstrates sufficiently high selectivity towards one of the components (for example, A) of the mixture being separated, then the separation can be achieved using "traditional" sequence of operations. This mode involves filtration of solution through the column with an ion exchanger until the breakthrough of component A followed by its elution from the resin by some auxiliary-stripping agent. Solution obtained after the first stage is either completely A-free or contain a far less A content.

The use of auxiliary reagent can be avoided if one can shift significantly the selectivity of resin by modulation of one of the physico-chemical parameters mentioned above. In this case the separated components can be eluted from the resin by solution of the same initial ionic composition. The first practical example of the single stage separation without auxiliary reagents refers to the softening of natural waters (or some other solutions) on a sulfonate resin using a more concentrated solution of the same ionic composition (containing the same monovalent and divalent ions) for regeneration of the resin [32]. The selectivity of resin towards $Mg^{2+}$ and $Ca^{2+}$ vs $Na^{+}$ from solution of higher concentration is lower than that from the dilute solution. Hence, this brine from the resin previously equilibrated with dilute solution elutes the significant part of magnesium and calcium ions. This technique is widely used at some power stations where the regeneration of strong acid resin is carried out using, e.g. seawater [33, 34].

During a long time the group of ion-exchange separation methods using the temperature induced shift of resin selectivity attracted the attention of scientists and engineers. The most well known in this group is the

Sirotherm process which is used for partial demineralization of natural waters [9-11]. Special ion-exchange resins which contain both weakly acidic and weakly basic functional groups are usually applied within this process. These resins sorb alkali metal salts from solution being treated at low temperature and desorb them by passing the same solution at high temperature. In the recent work [35] a similar process has been applied for a partial removal of calcium from the boiler water using a Sirotherm-10 resin.

In recent years several dual-temperature ion-exchange systems applicable for purification of highly concentrated alkali metal salt solutions from alkali-earth and transition metal ions have been discovered [12, 14, 36-39]. These systems involve polyacrylic and polymethacrylic resins, which increase significantly their selectivity towards divalent vs monovalent (alkali metal) ions with temperature.

The example of a single-stage dual-parametric operation using one of these resins is presented in Fig. 1. About 60 ml of polymethacrylic ion exchanger KB-4 (with 6% DVB) was first equilibrated in column at 20° C with a stock solution containing 2.5 N NaCl; 0.02 N $CaCl_2$ and 0.001 N $NiCl_2$. Then the same solution was filtered through the column at 78° C. Due to the higher selectivity of the resin towards divalent ions at high temperature a large volume of the effluent contained less calcium and nickel than the initial solution. Then the ion-exchanger was regenerated by the same initial solution at 20° C. At this stage the "excessive" amount of divalent ions was eluted from the ion exchanger so that their concentrations in the effluent obtained were significantly higher than those in the initial solution [38]. After this operation the purification-regeneration cycles were repeated. Analogous results were obtained earlier for purification of 2.5-5.0 N solutions of alkali metal salts from $Ca^{2+}$ admixture [36,37].

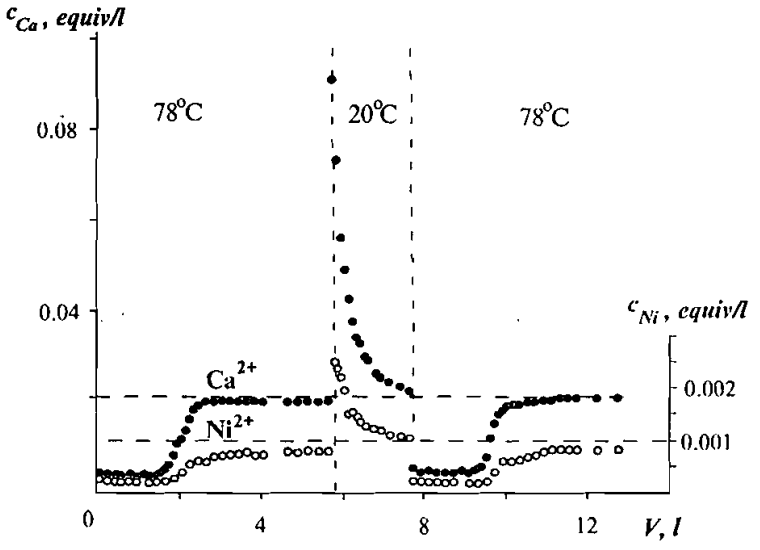


FIGURE 1. Breakthrough curves of dual-temperature single-stage purification of 2.5 N NaCl from 0.02 N $CaCl_2$ and 0.001 N $NiCl_2$ on polymethacrylic resin KB-4; height of resin bed = 81.5 cm; solution flow-rate = 5.5 cm/min [38].

Single-stage process can be carried out in a continuous mode using two counter-current columns operating at different temperature [39]. The flow-sheet of this process is presented in Fig.2a. The purification of solution from divalent ions is carried out in the "hot" column 1, while the regeneration of the resin proceeds in the "cold" column 2. The counter-current mode of operation allows purification of a larger volume of solution with the same amount of ion exchanger as comparison with the respective fixed bed process. It also requires a smaller amount of the initial solution to achieve the same degree of the ion exchanger regeneration.

Figs. 2b, 2c and 2d demonstrate the *y-x* diagram (McCabe-Thiele diagram) of the continuous process. The content of divalent ion in the initial solution feeding the "hot" column is some greater than that in the solution

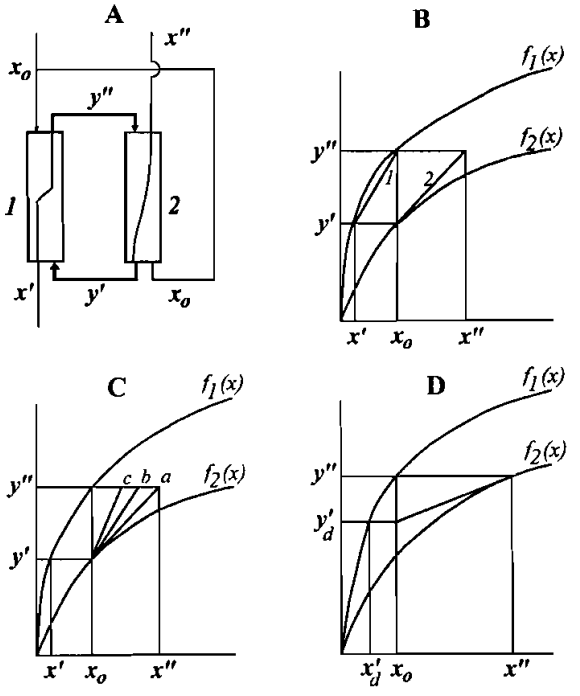


FIGURE 2. Flow-sheet (A) and *y-x* diagrams (B, C and D) of continuous dual-temperature single-stage purification from stronger sorbed impurities.

under equilibrium with the ion exchanger feeding the same column, $x_0 > g_1(y')$. It means that in the "hot" column of sufficient height the steady-state sorption front between solutions with concentrations of divalent ion $x_0$ and $x'$ is formed [40]. Operating line of this process is line 1 in Fig.2b. Its slope equals to the ratio of flows of ions being separated with the solution, $L_1 = \chi v c_0$, and the resin phases, $S = (1-\chi) w m_0$. This ratio can be defined as follows:

$$\frac{L_1}{S} = \frac{y' - y''}{x_o - x'} \tag{4}$$

where $v$ and $w$ are the linear flow velocities of solution and resin phases, respectively; $c_0$ and $m_0$ are the total concentrations of the separating ions in the solution and resin phases, respectively; $\chi$ is the void fractional volume of the resin bed.

When the stationary distribution of the ion concentrations along the "cold" column is achieved, the concentration of divalent ion varies monotonically from $x_0$ to $x''$. The equilibrium situation in the "cold" column suggests $y'=f_2(x_0)$. The minimal flow of the solution must correspond to the operating line which is the tangent to the equilibrium line $f_2(x)$ at the point $x_0$, so that the flow ratio $L_2/S$ must equal to the slope of this tangent [41]. The increase of the flow of regenerating solution, $L_2$, at the fixed resin flow, $S$, corresponds to the change of the position of operating line from "a" in Fig. 2c to "b" and "c" and does not lead to the change of composition of the product solution, ($x'$).

The decrease of flow $L_2$ causes the decrease of slope of the operating line (see Fig. 2d), and the maximal regeneration of the resin (up to $y'$) cannot be achieved. As the result the concentration $x'_d$ in the product solution is higher than that under the optimal conditions, i.e. $x'_d > x' = g_1(y')$. This means that the operating conditions, which correspond to the operating line (that is the tangent to the "cold" equilibrium line 2 at point $x_0$) are the optimal ones. Note that the above discussion is valid when both columns are of sufficient height, i.e. the number of theoretical plates in each column must equal to several tens.

The concentration of divalent ion in the regeneration effluent of column 2, $x''$, can be calculated as follows: the amount of divalent ion additionally sorbed by the resin in column 1 is $S(y''-y')=L_1(x_0-x')$. The complete regeneration suggests $y'=f_2(x_0)$, i.e. the same amount of this

component must be desorbed from the resin in column 2, that corresponds to the condition $L_1(x_0-x')=L_2(x''-x_0)$. From the definition of the operating line (see above) it follows that:

$$\left.\frac{df_2(x)}{dx}\right|_{x_o} = \frac{y''-y'}{x''-x_o} \tag{5}$$

This equation defines the concentration of the divalent ion, $x''$, in the regeneration effluent.

The decrease of the column length (or decrease the number of the theoretical plates), the operating line shifts away from the equilibrium line that results in the deterioration of separation.

Both periodical and continuous versions of the method under discussion make it possible to separate the initial solution into two parts. The first one is depleted with the divalent ion and the second one is enriched with the same component. The decrease of the divalent ions concentration in the purified solution which can be achieved on polymethacrylic and polyacrylic resins is usually about 6-10 times depending on the temperature dependence of the equilibrium characteristics of the resin. In the recent communication [42] the ion-exchange resins Lewatit R 249-K and Lewatit R 250-K of the same types have been successfully used for partial removal and concentration of calcium and magnesium ions from artificial and natural seawater. Several recent studies [43-48] report the results on application of iminodiacetic resins for the quantitative preparative single-stage separation of ionic mixtures containing $Cu^{2+}$, $Zn^{2+}$, $Al^{3+}$ and some other metal ions. In the last of the cited works the counter-current technique was used for dual-temperature separation of binary $Cu^{2+}$-$Zn^{2+}$ mixtures.

## 3. MULTIPLICATION OF SINGLE SEPARATION EFFECT

In most cases a single-stage (equilibrium) separation effects are not high enough to achieve a significant fractionation degree. Hence, a single-stage separation effect must be multiplied applying, e. g. a cascade of single-stage separation units, parametric pumping technique, or two-sectional columns operating in a dual-parametric mode.

### 3a. Parametric Pumping

Since the 70's this technique has been extensively studied and tested for separation of different ionic mixtures, but mainly on sulfonate resins [21-23]. The main feature of parametric pumping (PP) technique is the ability to use very small temperature shifts of resin selectivity to achieve sufficiently high separation degrees. Schematically, the PP separation process is shown in Fig.3a. A portion of the initial solution to be purified is passed at high temperature through a column with ion-exchange resin pre-equilibrated with the same solution at low temperature. Then the collected effluent is passed in the opposite direction at low temperature through the same column. This cycle is repeated for the collected fraction of solution in the same column. The effluent collected at one edge of the column is being enriched from cycle to cycle with one of the components, and the effluent collected at another edge is enriched with another one. The mechanism of PP separation is given in detail in numerous publications [see, e.g. 21-23] and will not be discussed here.

The PP technique was used for ion-exchange separation (on sulfonate resins) of different ion mixtures such as, $K^+$-$H^+$ and $K^+$-$Na^+$-$H^+$ [49]; $Ca^{2+}$-$K^+$[50, 51], and $Cu^{2+}$-$Ag^+$ [52, 53]. It was also applied for desalination of water on the retardation-type resin [54-56] and for separation of amino acids

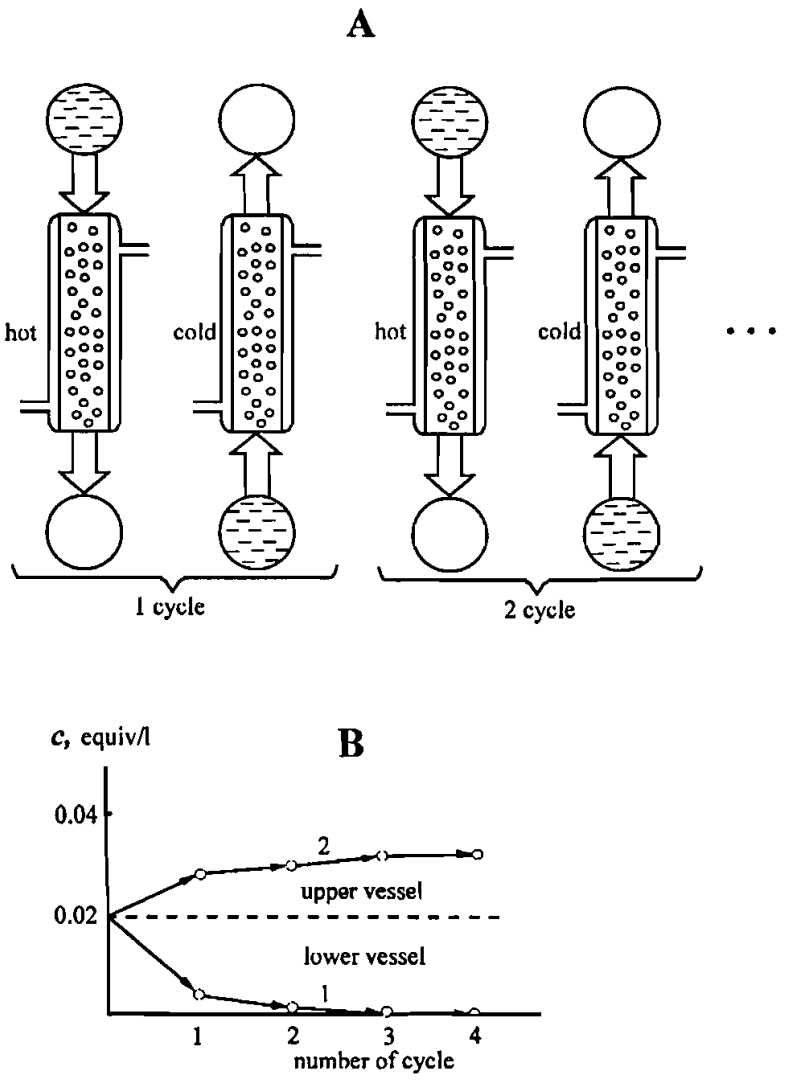


FIGURE 3. Schematic diagram of parametric pumping separation process: (A) sequence of operation cycles; (B) dependence of $Ca^{2+}$ concentration on number of "hot" (1) and "cold" (2) cycles. Initial solution: 2.5 N NaCl + 0.02 N $CaCl_2$ ; volume of solution 2000 ml; polymethacrylic resin KB-4; height of resin bed = 81.5 cm; resin bed capacity = 140 mequiv; solution flow-rate = 2.5 cm/min; $T_{hot}$ = 76°C and $T_{cold}$ = 10°C [36; 37].

[60]. In all cases the temperature-induced changes of the resin selectivity were small, and for achievement of significant separation degrees many cycles (up to 100) were needed. The PP technique has been developed in different operation modes such as periodic [49]; continuous [59]; recuperative [57], and cyclic zone [60, 61].

The ion-exchange PP purification of the alkali metal salt brines (with concentration from 2.5 to 5.0 equiv/l) from the alkali-earth and transition metal ions on polyacrylic and polymethacrylic resins have been described recently [36-39]. Two examples of the PP purification of NaCl solution are presented in Fig.3b and in Table 1. It is seen that the decrease of impurities content by a factor of $\sim 10^3$ is achieved within 5 cycles.

### 3b. Cascades of Single-Stage Separation Units

The theory of cascades of single-stage separation units (CSSSU) was created in 40's and 50's for the separation of isotope mixtures and was described for the first time in the Cohen monograph [62]. The main principles concerning the optimal design of cascades given in this book appear to be also valid (at least partially) for the ion-exchange and allied separation methods as well. To make this conclusion clearer let us consider CSSSU for separation of di- and monovalent ions using the ion-exchange system including polymethacrylic resin mentioned above (see Fig. 4). In the CSSSU such as, e.g. fixed bed or counter-current columns (see above), the purified solution after the first stage ("hot") is directed to the second "hot" stage (identical to the first one), then to the third (also "hot"), etc. The separation degree of solution components increases gradually from stage to stage. A fraction of solution after each "cold" stage containing increased concentration of divalent ions is added to the feed solution of the previous stage.

TABLE 1. PP PURIFICATION OF 2.5N NaCl SOLUTION FROM 0.02N $CaCl_2$ AND 0.001N $NiCl_2$ ON KB-4P2 RESIN.

| No. Cycle | Purification | | | | Regeneration | |
|---|---|---|---|---|---|---|
| | $c_{Ca}$, equiv /l | $c_{Ni}$, equiv /l | Purification degree $\varphi = c_o/c_l$ | | $c_{Ca}$, equiv /l | $c_{Ni}$, equiv /l |
| | | | $\varphi_{Ca}$ | $\varphi_{Ni}$ | | |
| 1 | $4.28\times10^{-3}$ | $2.2\times10^{-4}$ | 4.91 | 4.55 | 0.0318 | $1.18\times10^{-3}$ |
| 2 | $1.11\times10^{-3}$ | $0.85\times10^{-4}$ | 18.9 | 11.8 | 0.035 | $1.16\times10^{-3}$ |
| 3 | | | | | 0.036 | $1.25\times10^{-3}$ |
| 4 | | | | | 0.036 | $1.75\times10^{-3}$ |
| 5 | $3.75\times10^{-5}$ | $0.25\times10^{-5}$ | 533 | 400 | | |

Capacity of resin bed = 150 mequiv; column i. d. = 1.2 cm; volume of solution = 1500 ml; solution flow rate = 5.5 cm/min; $T_1$=78° C, $T_2$=20° C [38].

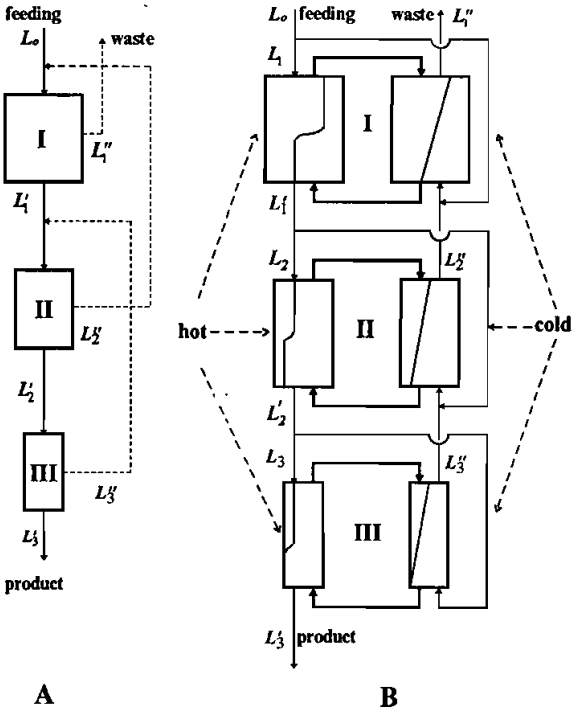


FIGURE 4. Ideal cascade of single-stage separation units for concentration of weaker sorbed component: (A) general flow sheet; (B) detailed flow sheet of ideal cascade of dual-parametric stages I, II and III by using counter-current columns.

The evolution of composition of the solution under purification flowing from stage *i-1* to stage *i* is characterized by the enrichment coefficient, $\beta_i$, which can be written for the purification the weaker sorbed ion from the stronger sorbed one as follows:

$$\beta_i = \frac{1-x_i}{x_i} \Big/ \frac{1-x_{i-1}}{x_{i-1}} \tag{6}$$

In order to use most effectively the separating power of each single stage it is expedient to design the cascade so that solutions of the same compositions are combined (so-called "ideal" cascade). Hence, the combined flows of the ideal cascade have the same compositions ($x'_{i-1}=x''_{i+1}=x_i$) at

$$\Theta_i = \frac{L'_i}{L'_i + L''_i} = \frac{1+(1-x_i)(\beta-1)}{\beta+1} \tag{7}$$

Here all $\beta$ values are equal for all stages. A more complicated result is obtained for the case when $\beta_i$ values vary from stage to stage:

$$\Theta_i = \frac{L'_i}{L'_i + L''_i} = \frac{(\beta_{i-1}-1)}{\beta_i \beta_{i-1} - 1}[1+(\beta_i - 1)(1-x_i)] \tag{7a}$$

Another useful result, which follows from the theory of the ideal cascade, is the decrease of the flows (the amounts) of the mixture being separated from stage to stage. Fig. 5 shows schematically the *y-x* diagram of the ideal dual-parametric cascade. As seen, the operating lines corresponding to individual stages form two broken lines. One of them

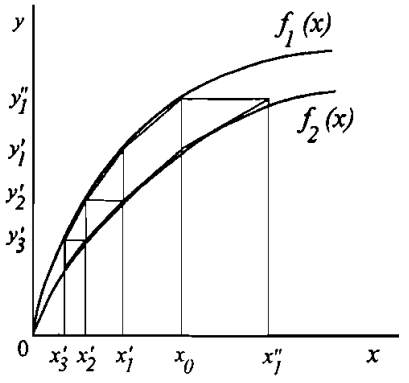


FIGURE 5. *y-x* diagram for ideal cascade of dual-parametric single-stages: $x_0$, $x_3'$ and $x_1''$ are equivalent fractions of stronger sorbed component in feed, product and waste solutions, respectively.

consists of a set of chords with common points located on the equilibrium curve $f_1(x)$ and corresponds to variation of the enriched (purified) flows. The other broken line consists of the segments of tangents surrounding the equilibrium curve $f_2(x)$. Cascade of the dual-temperature ion-exchange single-stage units used for the concentration of bromine from the seawater on a strong base anion exchanger is described in [63].

### 3c. Dual-Parametric Column

A counter-current column operating in a dual-parametric mode represents another tool for achievement of high separation degrees. The theory of the dual-temperature separation in two-sectional counter-current columns has been developed in detail since the 40's [64-67]. This separation technique was successfully applied for decades to produce $D_2O$ by chemical exchange in gas-liquid systems involving $H_2S$–$H_2O$ and $H_2$–$H_2O$ (dual-temperature method for deuterium concentration).

The flow-sheets and the *y-x* diagrams of different variants of dual-temperature concentration of deuterium by chemical isotope exchange in $H_2O$-$H_2S$ system was described in several reviews [68-72]. Nearly the same principles can be used for the dual-parametric ion-exchange separations and they will not be considered here in detail. Some features of separation in a simple dual-temperature column at non-linear equilibrium dependencies $y=f_1(x)$ has been discussed in [73]. Thus it has been shown that from respective *y-x* diagram one can determine the limited value of separation degree in a given system which corresponds to the composition at the point of intersection of the operating line and the equilibrium curve. In order to increase the efficiency of separation a change of the flows ratio in certain parts of cold and hot sections has been proposed. For thisapproach a part of one of the contacting flows is withdrawn from some point of hot column and is redirected to the respective point of the cold column where the composition of the same phase is identical. Later similar operation modes were also described in [31] where a detailed consideration of the flow-sheets and *y-x* diagrams for the dual-temperature processes at non-linear equilibrium dependencies were presented.

Reagent-less ion-exchange separation in a two-sectional column with moving boundary between two temperature zones on a simulated moving bed of a sulfonate cation exchanger has been experimentally studied for the first time for separation of $Li^+$-$NH_4^+$ and $Cs^+$-$Na^+$ mixtures [24, 25]. However, separation in the dual-temperature simulated moving bed column appeared to be too complicated and has not found any further development. Later [29, 30], the dual-temperature separation of $Ca^{2+}$-$K^+$; $Na^+$-$H^+$, and $Fe^{3+}$-$Cu^{2+}$-$H^+$ mixtures in counter-current columns with the counter-flow of both solution and resin (sulfonate) phases has been investigated.

The idea of dual-temperature-like ion-exchange counter-current separation in two-sectional columns based on the shift of resin selectivity by modulation of other physical-chemical parameters (other than temperature) originated in 1970 in Moscow State University by Gorshkov et al. [26]. The group of these separation techniques is known as dual-parametric mode by analogy with dual-temperature separation. Another version of the reagent-less separation process combines the dual-parametric separation with the partial flow reversal. This separation mode is known as the "combined scheme" or "combined separation process" [74]. Some of the results obtained by experimental and theoretical studies of continuous separation processes in dual-parametric columns will be presented in the next part of this paper.

## 4. DUAL-PARAMETRIC SEPARATION

The dual-parametric separation is based on the alteration of certain physico-chemical condition (solution concentration, pH, etc.) in the column sections to provide the variation of the equilibrium coefficients in different sections. Fig. 6a shows schematically the flow-sheet of the dual-parametric separation of the stronger sorbed component from the binary mixture. The distribution of the target component along the column is shown in Fig. 6b. For comparison, Fig.6c presents the flow-sheet of conventional ion-exchange separation with the use of auxiliary stripping reagent, D, for displacement of the mixture components from the resin. The fractionation technique shown in Fig. 6b, is known as continuous reverse frontal separation or reverse frontal chromatography. The displacement process can be characterized in terms of the general theory of separation as *"flow reversal"* that is, identical to, e.g. "reflux" in distillation.

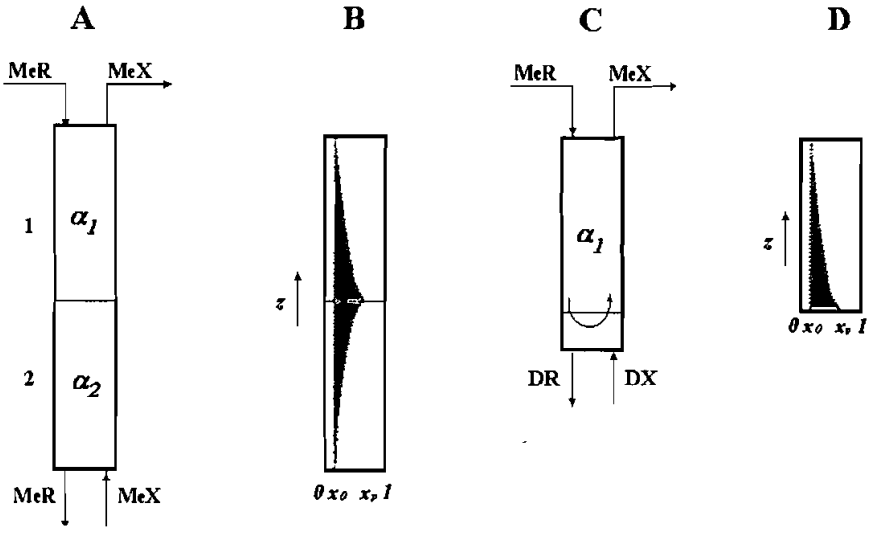


FIGURE 6. Concentration of stronger sorbed component in dual-parametric process (A, B) and in process with flow reversal (C, D): (A, C) process flow-sheets; (D, B) schematic distributions of concentrated component along column heights. Me is mixture of separated ions; X is anion; R is polymeric matrix with functional groups; D is auxiliary cation (displacer).

As seen in Figs. 6a and 6c, in both cases the columns are fed with the ion exchanger pre-loaded with the mixture under separation, MeR, from the top. As seen in Fig. 6d, where the distribution of the component being concentrated along the column is shown, the accumulation of this component proceeds near the flow reversal point.

The upper section of the dual-parametric column (see Fig. 6a) is analogous to the separation section of the column in Fig. 6c, while the bottom section in scheme 6a replaces the part of the column in scheme 6c where the flow reversal occurs. The ion exchanger from section 1 passes into section 2 while the initial solution of the separated ions, MeX, is fed

into the bottom of section 2. The conditions in sections are maintained so that the equilibrium separation coefficient (see eq. 1) $\alpha_2$ is less than $\alpha_1$. In this case, the ion-exchange resin equilibrated with the initial solution in sections 1 and 2, must contain different fractions of the component being separated. The excessive amount of this component in the resin in section 1 as compared with that in section 2 is determined by the difference between $\alpha_1$ and $\alpha_2$. This excess is eluted from the ion exchanger at the boundary between sections and returns back in section 1. The accumulations of the target component proceeds near the boundary between sections of the counter-current column (see Fig. 6b) and gradually increases.

As follows from the theory of dual-temperature method [65, 66], the separation efficiency depends on the difference in $\alpha_1$ and $\alpha_2$ values, that is also valid for the dual-parametric separation. Moreover, both dual-temperature and dual-parametric separation processes are characterized by a strong dependence of the separation degree on the ratio of feed flows entering the column with the resin and solution phases, which is characterized by a sharp maximum corresponding to the optimum conditions (see below).

### 4a. Dual-Parametric Separation Based on Variation of Resin Selectivity with Solution Concentration.

The separation processes described in this section allow using the close-cycle flow of the ion exchanger that minimizes the required investment of the resin. Fig.7 shows a flow-sheet of separation process based on the change of ion-exchanger selectivity with solution concentration [26, 27, 75, 76]. The selectivity changes are particularly high for the exchange of ions with different charges. The separation is carried out in two-sectional counter-current column. The ion exchanger loaded with the

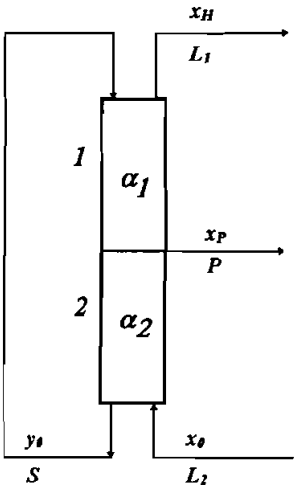


FIGURE 7. Schematic diagram of dual-parametric separation with closed circulation of ion exchanger based on alteration of solution concentration at boundary between sections.

ions to be separated moves from the top to the bottom and after leaving the column, directed back to the upper section without any treatment. The solution containing the same ions is fed into the bottom of the column and is removed from the top. At the boundary of sections either dilution or concentration of solution is accomplished.

In the beginning of the operation cycle, the composition of ion exchanger leaving the column is characterized by $y_0$ value which corresponds to the equilibrium with feeding solution of composition $x_0$. Hence, the equilibrium in section 2 can be described by eq. 1 as follows:

$$\alpha_2 = \frac{y_0}{1-y_0} \cdot \frac{1-x_0}{x_0} \tag{1c}$$

The composition of ion exchanger being fed into the top of the column, $y_0$, and that of the solution leaving section 1, $x_H$, are also connected with each other by the equilibrium condition:

$$\alpha_1 = \frac{y_0}{1-y_0} \cdot \frac{1-x_H}{x_H} \tag{1d}$$

From equations 1c and 1d one obtains:

$$\frac{x_H}{1-x_H} = \frac{\alpha_2}{\alpha_1} \cdot \frac{x_0}{1-x_0} \tag{8}$$

A similar result is obtained by using eq. 2 for the exchange of di- and monocharged ions:

$$\frac{x_H^{1/2}}{1-x_H} = \frac{K_2}{K_1} \cdot \frac{x_0^{1/2}}{1-x_0} \tag{9}$$

The selectivity of resin (e.g., sulfonate) towards ions of bigger charge is higher in dilute solution than in a more concentrated one. Hence, if solution is diluted, e.g. at the boundary of sections, then $K_2<K_1$; $x_H<x_0$, and the ions of bigger charge are accumulated in the column. In the opposite situation, i.e. when solution is concentrated at the boundary of sections, $K_2>K_1$, and the ions of smaller charge must be accumulated in the column.

The selectivity coefficient $K$ (see eq. 2) can be expressed through the concentration equilibrium constant $\tilde{\tilde{K}}$ as follows: $K = \tilde{\tilde{K}} \cdot \left(\frac{m_0}{c_0}\right)^{1/2}$. Hence, if both $\tilde{\tilde{K}}$ and $m_0$ do not depend on the concentration of solution then from (9) one obtains:

$$\frac{x_{\mathrm{H}}^{1/2}}{1-x_{\mathrm{H}}} = \left(\frac{c_{0,1}}{c_{0,2}}\right)^{1/2} \cdot \frac{x_0^{1/2}}{1-x_0} \tag{9a}$$

Equation 9a can be simplified for small $x$ values, i.e. when $x_H$<<1 and $x_0$<<1 as follows:

$$x_H = \frac{c_{0,1}}{c_{0,2}} \cdot x_0 \tag{3d}$$

The estimate of the range of ion flows ratio entering the dual-parametric column with solution, $L=\chi v c_0$, and with ion exchanger, $S=(1-\chi)wm_0$, phases corresponding to effective separation can be based on the following considerations: the necessary condition for a component to be concentrated is that at the initial period of operation cycle the amount of this particular component entering the column with one of the phases (e.g., solution) should be larger than its amount leaving the column with the other phase (e.g., resin). The following inequalities should be fulfilled: $L_2 x_0 > S y_0$ and $L_1 x_H < S y_0$. If the column is working in the "without-product-withdrawal" mode of operation, then $L_2=L_1=L$, and the above inequalities can be rewritten as follows:

$$\frac{y_0}{x_0} < \frac{L}{S} < \frac{y_0}{x_{\mathrm{H}}} \tag{10}$$

The difference between compositions of phases is maximal at the beginning of the column operation cycle when the inter-phase equilibrium prevails at the edges of the column. For the linear equilibrium relationship, i.e. when $y=\alpha x$, from eq. 10 one obtains:

$$\alpha_2 < \frac{L}{S} < \alpha_1 \tag{11}$$

Similarly, for concentration of the second component (when $1-y=(1-x)/\alpha_i$,) must proceed if the following inequalities are fulfilled:

$$\frac{1}{\alpha_2} < \frac{L}{S} < \frac{1}{\alpha_1} \tag{12}$$

As will be demonstrated below, relations (11) and (12) can be fulfilled only for the initial period of the dual-parametric column operation. At the steady-state regime the inter-phase equilibrium at both edges of the column can occur only when the product is being withdrawn, i.e. in this case $L_1 \neq L_2$.

The process shown in Fig. 7, was used for separation of $Ca^{2+}$ and $K^+$ from 0.7N solution containing either 5% or 50% KCl [26, 27] in the counter-current column (i.d 2.6 cm; height of 220 cm) with continuous movement of the resin under gravity and the counter-flow of solution. The construction of experimental set-up used was similar to that described in [77]. The unit was provided with the facilities for injecting water in the middle part of the column. The sulfonate cation exchanger, KU-2x9, pre-equilibrated with the initial solution, was fed into the top of the column and moved downwards. The stock solution was fed into the bottom part of column. Water was injected continuously into the middle part of the column at a flow rate providing the dilution of the initial solution from 0.7 to 0.17 N in the upper section. This caused the variation of $\alpha_K^{Ca}$ values from 2.0 to 4.7 for the mixture containing 5% KCl.

Fig. 8 shows the experimentally determined distributions of separated ions along the column at different periods for the initial mixture containing 50% KCl. After achieving the steady state the solution containing less than

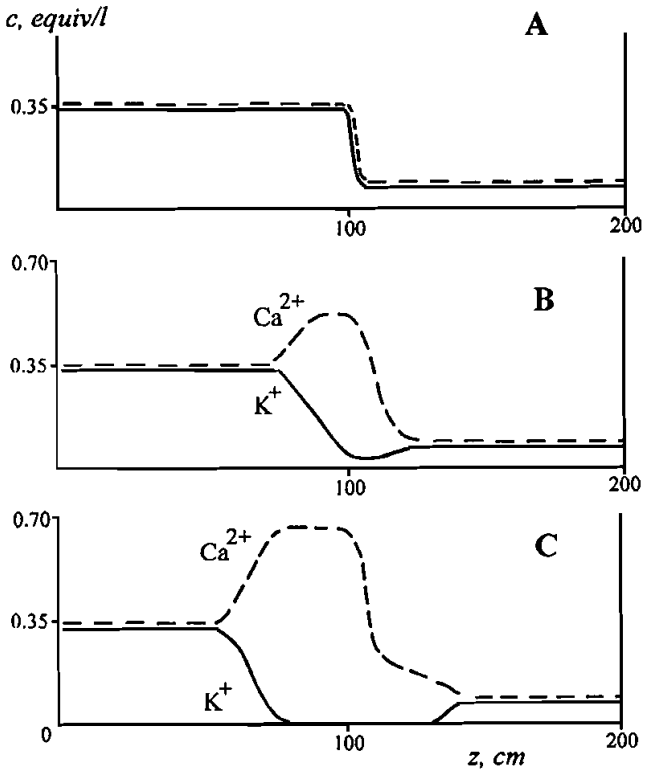


FIGURE 8. Experimentally determined concentration-coordinate along column histories of dual-parametric separation of $Ca^{2+}$ and $K^+$ on sulfonate ion exchanger KU-2x8 (see text). Conditions: $c_2 = 0.7$ equiv/l; $x_0 = 0.5$; solution flow-rate = 0.38 cm/min; resin flow-rate = 0.1 cm/min; time of column operation (hours): 0 (A); 22 (B); 70 (C) [26; 27].

0.01% KCl was withdrawn from the middle part of the column. Similarly, the accumulation of $K^+$ was carried out in experiments based on the opposite change of resin selectivity due to the concentration of solution (see above). For this, solution leaving the bottom section (see Fig.7) was partially evaporated prior entering the upper section [75].

As follows from the theory of dual-temperature separation for the linear equilibrium isotherms [65, 66], for concentration of the component

with weakest sorbability in the "without-product-withdrawal" mode (when $L_1=L_2=L$), the optimal value of flows ratio in the column can be found from the following expression:

$$\left(\frac{L}{S}\right)_{opt} = \frac{\alpha_1 N_1 + \alpha_2 N_2}{N_1 + N_2} \tag{13}$$

Here $N_1$ and $N_2$ are the numbers of transfer units (similar, to some extent, to theoretical plates) in sections. A similar equation can be derived for the concentration of a stronger sorbed component. Equation (13) is modified in this case so that $\alpha_1$ and $\alpha_2$ are substituted by $1/\alpha_1$ and $1/\alpha_2$., respectively. These relationships were confirmed by the experimental results [76] obtained by purification of $CaCl_2$ from KCl. Some of these results are shown in Table 2. The kinetics of the process carried out at *L/S* values close to the optimal is presented in Fig.9. In all experiments $Ca^{2+}$ was accumulated in the middle part of the column. When dilution factor achieves 4.5 - 5.5, the dependence of maximum (steady-state) separation degree $q=x/x_0$ vs *L/S* is characterized by a bell-like curve with the maximum at *L/S* values between 0.5 and 0.6. Thus, the optimal flows ratio is close to the slope of the equilibrium line for the $Ca^{2+}$-$K^+$ exchange from 0.7N solution ($1/\alpha$=0.53). This result is in agreement with that determined theoretically from eq. 13. Indeed, the solution flow-rate in the upper section is far higher than that in the bottom one (due to dilution). Hence, the height of the transfer unit (HTU) in the upper section is much higher than that in the bottom. Consequently, $N_1 << N_2$, and $\left(\frac{L}{S}\right) \approx \frac{1}{\alpha_2}$.

The comparison of the curves describing $q$ vs. distance along the column, $z$, allows some conclusions regarding the kinetics of the process to be drawn. For example, in experiment N6 where *L/S* ration is close to the optimal value (see Fig.9) the $q$ vs $z$ curves are symmetric with respect to the boundary of sections and the separation degree gradually increases in time.

TABLE 2. PURIFICATION OF $CaCl_2$ FROM KCl (19:1) ON KU-2x9 RESIN [76].

| No. | Phase flow rate, ml/hr | | | Dilution factor | Operation time, hrs | $L/S$ | $q_{max}$ |
|---|---|---|---|---|---|---|---|
| | Solution (0.7N) | Resin | Water | | | | |
| 1 | 64.0 | 23.5 | 229 | 4.6 | 140 | 0.95 | 14 |
| 2 | 55.3 | 22.2 | 227 | 5.1 | 69 | 0.87 | 30 |
| 3 | 46.6 | 23.0 | 208 | 5.5 | 96 | 0.74 | 90 |
| 4 | 40.9 | 23.4 | 141 | 4.5 | 150 | 0.61 | >4000 |
| 5 | 37.4 | 23.2 | 151 | 5.0 | 104 | 0.56 | 500 |
| 6 | 72.5 | 42.7 | 237 | 4.4 | 200 | 0.60 | >4000 |
| 7 | 56.1 | 44.7 | 220 | 4.9 | 77 | 0.44 | 560 |
| 8 | 35.2 | 45.6 | 135 | 4.8 | 50 | 0.27 | 10 |
| 9 | 42.2 | 23.8 | 87 | 3.1 | 170 | 0.62 | >4000 |
| 10 | 42.4 | 23.5 | 48 | 2.1 | 250 | 0.63 | 29 |
| 11 | 42.3 | 23.1 | 33 | 1.8 | 270 | 0.64 | 13 |

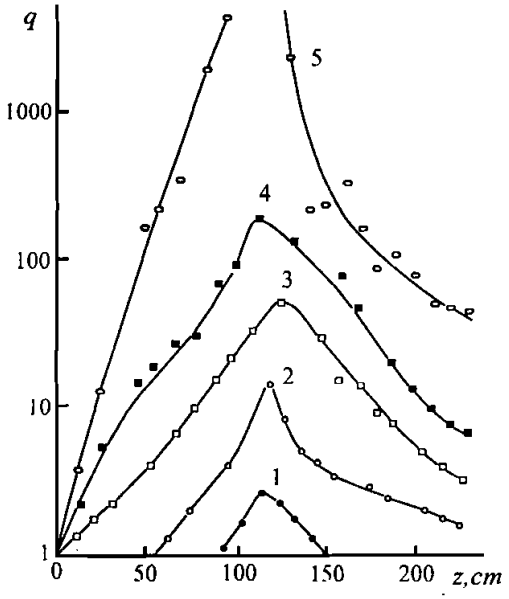


FIGURE 9. Experimental plots of separation degree $q = x/x_o$ versus coordinate along column ($z$) for 4 (1); 11 (2); 28 (3); 49 (4), and 97 hours (5) of column operation at optimal flows-ratio (see text). Conditions: sulfonate resin KU-2x9, $c_2 = 0.7$ equiv/l; $x_o = 0{,}95$; solution flow-rate = 0.62 cm/min; resin flow-rate = 0.24 cm/min; water injection rate = 1.95 cm/min [76].

At $L/S>(L/S)_{opt}$ calcium is concentrated mainly in the upper section of the column while in the bottom section the ionic composition remains close to the initial one (see Fig.10). At $L/S < (L/S)_{opt}$ the zone enriched with calcium is shifted to the bottom section. As the result, the more is the deviation of ***L/S*** from the optimal value, the lower the $q$ vs $z$. curves lie. This criterion can be used to determine the direction of possible deviation of the chosen flows ratio from the optimal value.

The results shown in Table 2 for experiments No.9-11 (see also No.4) illustrate the influence of dilution factor (or $\alpha_1$ - $\alpha_2$ value) on the efficiency of purification process. In these experiments the flows ratio was kept constant at $L/S\approx0.6$ level while at constant flow values the degrees of solution dilution were different. The decrease of dilution factor from 4.5 to 3.1 resulted in a small shift of the purified product zone downwards while the maximal purification degree $q_{max}$ remained almost constant in different experiments. At the same time, the subsequent decrease of dilution to 2.1 or 1.8 resulted in a sharp drop of $q_{max}$ due to the further shift of the purified zone down. The main reason for the observed effects was the decrease of $(\alpha_1-\alpha_2)$ value that resulted in the restriction of the interval of flows ratio where the effective separation proceeds.

The combination of two dual-parametric counter-current columns, in one where both the dilution and concentration of solution are carried out, enables one to design the process for recovery of both components of the mixture in a pure state. In this process the solution leaving one of the columns is fed to the other one. No auxiliary ions are required either for separation or for regeneration of the ion exchanger. The dilution and concentration of solution and reconciliation of the solution flows are the only auxiliary operations to be fulfilled (see below Fig.12).

A similar scheme was also used in [29, 30] for continuous dual-temperature separations of $Ca^{2+}$-$K^+$, $Na^+$-$H^+$ and $Fe^{3+}$-$Cu^{2+}$ mixtures on a

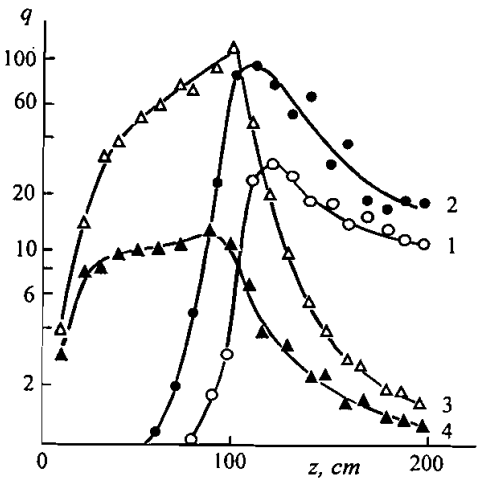


FIGURE 10. Experimental $q$ versus $z$ plots for different flows ratio, $L/S$: 0.87 (1); 0.74 (2); 0.44 (3); 0.27 (4) [76].

sulfonate ion exchanger. For example, the sequential treatment of 0.15 equiv/l $Ca^{2+}$ and 0.35 equiv/l $K^+$ solution at 4°C and 60oC allowed to obtain the product solutions with $x_{Ca}$=0.989 and $x_K$=0.013. This result was in a good agreement with the predictions based on the equilibrium theory of the percolation processes.

## 5. SEPARATION BASED ON VARIATION OF BOTH SELECTIVITY AND CAPACITY OF ION EXCHANGER. COMBINED SEPARATION PROCESS.

### 5a. Process Flow-Sheets

In this section the separation processes based on the dependence of both selectivity and capacity of polyfunctional ion exchangers on solution pH will be considered [28]. The ion-exchange processes on polyfunctional

resins bearing different functional groups are known to be pH dependent since the selectivity of different groups (e.g., of different acidity) towards the same ions differs, as a rule, in different pH ranges. For example, the ion-exchange equilibrium of cesium and rubidium on sulfo-phenolic cation exchanger KU-1 in neutral solution is characterized by $\alpha_{Rb}^{Cs} \approx 1.5$ while in the alkaline solution $\alpha_{Rb}^{Cs}$ grows to 2.0 [17,18]. In the last case the sorption capacity of the resin is 1.5-3.0 times higher than that in the neutral solution. For $K^+$-$Na^+$ exchange on the same resin an opposite trend is observed, i.e. the respective $\alpha$ values equal 1.5-1.8 in the neutral solution and drop to 1.2-1.4 in the alkaline media.

The flow-sheet of the separation process on a sulfo-phenolic resin is shown in Fig.11a. The ion exchanger pre-equilibrated with the mixture of ions to be separated from a neutral solution (so that only sulfonate groups appear to be loaded) is fed into the top of column and treated with alkaline solution of the same ionic mixture entering to the bottom part of the column. The protonated phenolic groups of the resin react with $OH^-$ and appear to be also loaded with metal ions to be separated. A rather sharp steady-state boundary between the alkaline and neutral solutions is formed in the column. When the flow of alkali (with solution phase) and that of phenolic groups of the resin equal to each other (in equivalents), the boundary remains stationary. The equilibrium separation coefficients $\alpha_1$ and $\alpha_2$ in the top and in the bottom sections differ from each other which creates the necessary conditions for the dual-parametric separation. Since the enrichment attainable depends on the ratio of the separated mixture flows, a mixture of salts is added to the feeding solution to regulate this parameter to obtain the desired magnitude of the flow ratio.

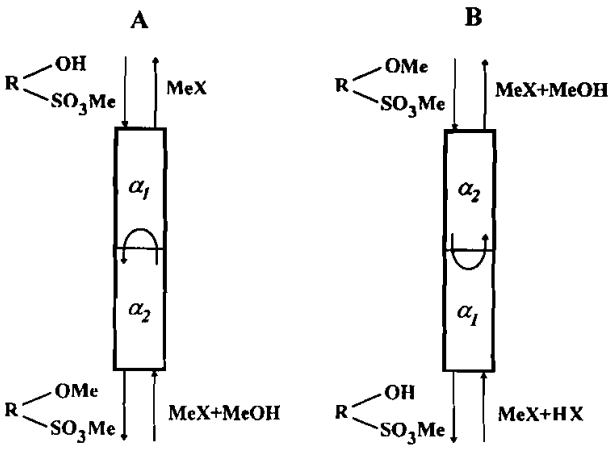


FIGURE 11. Schematic diagram of combined separation process based on alteration of selectivity and capacity of bi-functional (sulfo-phenolic) ion exchanger: (A) sorption of separated mixture by weakly dissociating (phenolic) groups; (B) partial desorption of separated ions.

A certain fraction of ions transfers from solution to the resin phase at the boundary between different pH zones due to the sorption on phenolic groups. *Hence, in this part of the column the separation process proceeds by the combined mechanism, involving both dual-parametric fractionation and separation with partial flow reversal*[1]. Later in the text processes of this type will be mentioned as combined separation processes. The separation with flow reversal must be accompanied by the concentration of the component of weaker sorbability in the upper part of zone 2. The "direction" of separation in dual-parametric method is determined by the difference of equilibrium separation coefficients $\alpha_1$ and $\alpha_2$. For example, for the $Cs^+$ and

[1] The idea of separation by combined scheme has been described for the first time in a general form in [74].

$Rb^+$ mixture the selectivity of sulfo-phenolic cation exchanger towards cesium in alkaline solution is higher than that in the neutral solution [17, 18], i.e., $\alpha_1<\alpha_2$. In this case the separation by dual-parametric mechanism follows the same direction as that of $Rb^+$ enrichment by separation with flow reversal.

In order to concentrate the second component of the mixture, a partial displacement of the separated ions from the resin (completely loaded with mixture components both by sulfonic and phenolic groups) is required (see Fig.11b). For this, one can use the acidified solution of separated ion salts. The steady-state front between acidic and alkaline solution zones is also formed in the column so that separation coefficients in these two zones are also different. Thus, two separation mechanisms appear to be combined in this case.

Fig.12 shows a process flow-sheet for the continuous recovery of both components of the mixture. A polyfunctional ion exchanger containing ions to be separated is passed successively through columns I and II and then is returned to column I without any additional treatment. Solution of the separated mixture circulates in the opposite direction. The pH of solution is changed prior to entering the columns to provide both additional sorption in column I (due to alkalization) and partial displacement of separated ions from a part of functional groups (e.g., weakly acidic) in column II (acidification). Separated components are collected from the middle parts of the columns and an additional quantity of the initial solution mixture is added to the input of column I.

Since the same amount of ion exchanger is circulating in columns, then $S_2$ and $S_1$ flows remain constant while the solution flow leaving one of the columns do not correspond to that providing the separation under optimum conditions in the other column. For this reason only a part of

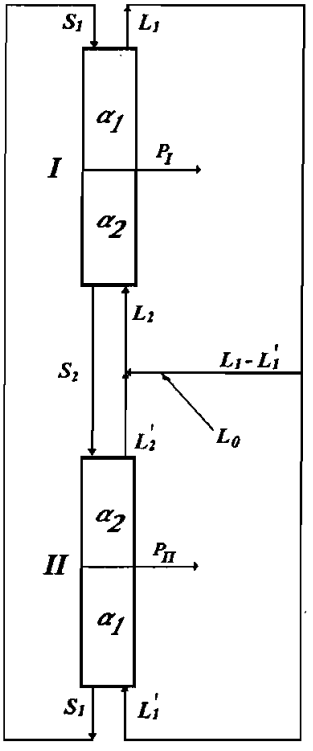


FIGURE 12. Schematic diagram of combined process for separation of two components from binary mixture.

solution flow leaving column I is utilized to feed column II while the remaining part is combined with solution feeding column I.

## 5b. Theory of Steady-State Process

The theory of separation using a combined separation process (CSP) was considered in detail in [78, pp.70-82; 77-79]. The theoretical description of the steady-state process within the one-dimensional non-equilibrium model of plug flows is based on the differential balance

equations written for section 1 and 2 (see Fig.13) as follows:

$$S_1 \frac{dy}{dz} = L_1 \frac{dx}{dz} = k_1[y - f_1(x)] \qquad \text{for } 0<z<H_1 \tag{14}$$

$$S_2 \frac{dy}{dz} = L_2 \frac{dx}{dz} = k_2[y - f_2(x)] \qquad \text{for } -H_2<z<0 \tag{15}$$

where $k_1$ and $k_2$ are the mass transfer coefficients.

The boundary conditions for the input of phases are defined in the following form:

$$y(H_1) = y_0 \tag{16}$$

$$x(-H_2) = x_0 \tag{17}$$

Different versions of CSP process are distinguished from each other by 1) the direction of the flux $F$ (from $S$ to $L$ or vice versa); 2) by the phase from which the product is withdrawn ($S$ or $L$), and 3) by the location of the product withdrawal point (above or below the boundary of sections). The mathematical models of different CSP are distinguished by different additional conditions. For example, in the process presented in Fig.13, the product is withdrawn with the solution phase from the point located just a bit below the point of partial flow reversal. Hence, the junction conditions for the boundary of sections (at $z$=0) are written as follows:

$$x(0-) = x(0+) \tag{18}$$

$$L_1 x(0+) = L_2 x(0-) - Px(0-) - Fx(0-) \tag{19}$$

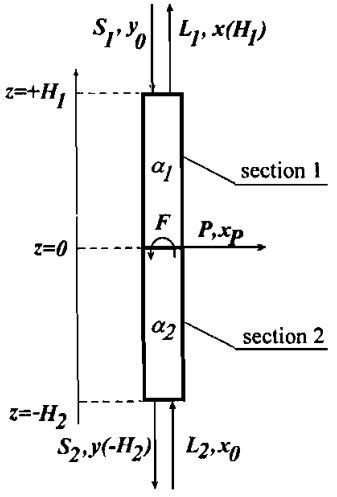


FIGURE 13. Schematic diagram of dual-parametric counter-current column with partial flow reversal on boundary between sections (see text).

where $P$, $L_2$ and $S_1$ are the controlled parameters of the process, and $F = S_2 - S_1$. The coordinates a bit below or above the boundary of zones are denoted here as $-0$ and $+0$.

At $F = 0$ we have a simple dual-parametric process (without partial flow reversal). For this case the solution of eqs. 14 - 19 for the linear isotherms was reported in [65,66]. For the CSP (when $F \neq 0$) with linear isotherms $f_i(x) = \alpha_i x$, and $y_o = \alpha x_0$ the analytical solutions of equations 14-19 have been published in [78, pp.79-80; 79; 82] and can be written in the following form [79]:

$$x_P = \frac{(a\alpha_2 - \gamma) - (\alpha_1 - \gamma_1)\alpha_1 \frac{1 - e^{+\mu_2}}{\alpha_1 - \gamma_1 e^{-\mu_1}}}{[(\alpha_1 - \gamma_1) - \frac{P}{S_1}\frac{(\alpha_1 - \gamma_1)\alpha_1}{\alpha_1 - \gamma_1 e^{-\mu_1}}] + [a\alpha_2 - (\alpha_1 - \gamma_1) - \gamma + \frac{P}{S_1}\frac{\alpha_1 - \gamma_1}{\alpha_1 - \gamma_1 e^{-\mu_1}}]e^{+\mu_2}} x_0 \qquad (20)$$

Here $\mu_1=N_1(\alpha_1 - \gamma_1)$; $\mu_2=N_2(\alpha_2 - \gamma_2)$; $a=S_2/S_1$; $N_1 = H_1k_1/S_1$ and $N_2 = H_2k_2/S_2$ are the numbers of the transfer units in two sections of column; $\gamma_i = L_i/S_i$ are the flows ratio in sections, and $\gamma=L_2/S_1$. The solution of the analogous model for purification of the stronger sorbed component (see flow-sheet in Fig.11b) was reported in [82]. These solutions allow examining the influences of different parameters on the separation process.

For the nonlinear equilibrium dependencies (described by, e.g. the mass action law) the numerical methods should be used to obtain the respective solutions. At the same time, some important qualitative results can be deduced by using the asymptotic approach [78; 79] described below for the flow-sheet of process shown in Fig.13.

For the column of fixed length the operating line in $y$-$x$ diagram (see Fig.14) for section 1 is located above the equilibrium curve $y = f_1(x)$ while for section 2 the operating line lies below the equilibrium curve $y = f_2(x)$. At the same time the equilibrium curve $f_1(x)$ can be located either below the equilibrium curve $f_2(x)$ (as shown in Fig.14) or above. Both equilibrium curves can also intersect each other or coincide with each other.

At the given values of equilibrium parameters and compositions of feeding phases ($x_0$ and $y_0$) the flows $S_1$ and $L_2$, and the flow of product withdrawal $P$, (or the ratios $\gamma=L_2/S_1$ and $P/S_1$) are variable. From the balance equation

$$L_2 - S_2 - L_1 + S_1 - P = 0 \tag{21}$$

the following relationship between $\gamma=L_2/S_1$; $\gamma_1=L_1/S_1$, and $\gamma_2=L_2/S_2$ can be derived:

$$\gamma=a\gamma_2=\gamma_1+(a-1)+P/S_1 \tag{22}$$

where $a \equiv S_2/S_1$.

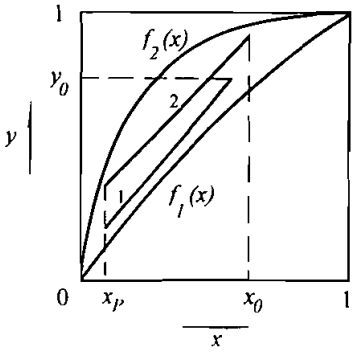


FIGURE 14. $y$-$x$ diagram of two-sectional column shown in Fig. 13. (1) and (2) are operation lines in sections.

At the steady-state operation of column the following mass balance and operation line equations are valid:

$$L_2 x_0 - S_2 y(-H_2) - L_1 x(H_1) + S_1 y_0 - P x_p = 0 \tag{23}$$

at z >0 $$L_1 x - S_1 y = C_1 \tag{24a}$$

at z < 0 $$L_2 x - S_2 y = C_2 \tag{24b}$$

where constants $C_1$ and $C_2$ can be found from the composition of phases in some parts of the column.

The asymptotic approach suggests that, at the limitless increase of section heights, the operating lines pass near the corresponding equilibrium curves until the operating line of section 2 intersects the equilibrium line $y=f_2(x)$, and the operating line of section 1 coincides with the tangent to the equilibrium line $y=f_1(x)$ or intersects it. This means that in intersection

points of operating and equilibrium lines, or in the region where operating and equilibrium lines nearly touch each other, the composition of phases nears that at equilibrium [40; 41; 83]. This makes it possible to find constants $C_1$ and $C_2$ (see equations 24a and 24b) using respective equilibrium dependencies and to express the composition of phases leaving sections (see equation 23), $y(-H_2)$ and $x(H_1)$, through the following parameters: $\gamma_1$ ; $\gamma_2$; $x_0$; $y_0$, and $x_P$.. The equilibration conditions of phases at the edges of sections are written as follows [see 78, p.43; 83]:

**Section 1:**

$$\gamma_1 \le \frac{df_1(x)}{dx}\Big|_{x=g_1(y_o)} \tag{25}$$

$$\gamma_1 \ge \frac{df_1(x)}{dx}\Big|_{x=x_P} \tag{26}$$

**Section 2:**

$$\gamma_2 \le \frac{f_2(x_0)-f_2(x_P)}{x_0-x_P} \tag{27}$$

$$\gamma_2 \ge \frac{f_2(x_0)-f_2(x_P)}{x_0-x_P} \tag{28}$$

The equilibrium, e.g. in section 1 cannot be achieved either in the top or in the bottom part if flow ratios lie within the following interval:

$$\frac{df_1(x)}{dx}\Big|_{x=g_1(y_0)} < \gamma_1 < \frac{df_1(x)}{dx}\Big|_{x=x_P} \tag{29}$$

In this case at the limitless length of section 1 the operating line coincides with the tangent to the equilibrium curve in some *intermediate* point $\bar{x}_1$ (where the equilibrium is achieved, i.e. $\bar{y}_1 = f_1(\bar{x}_1)$) determined from the following condition:

$$\gamma_1 = \left.\frac{df_1(x)}{dx}\right|_{x=\bar{x}_1} \tag{30}$$

The limiting situations, which can be achieved in two-sectional column with endless section lengths, are summarized in Table 3 for positions of equilibrium curves shown in Fig.14. As seen from (25)-(29) the interval limits for the ratio of flows feeding the column $\gamma = L_2 / S_1$ which correspond to one of the situations "a - f" (see Table 3) are determined by the following equations:

$$\gamma = a\frac{f_2(x_0) - f_2(x_P)}{x_0 - x_P} \tag{31}$$

$$\gamma = \left.\frac{df_1(x)}{dx}\right|_{x=x_P} + (a-1) + \frac{P}{S_1} \tag{32}$$

$$\gamma = \left.\frac{df_1(x)}{dx}\right|_{x=g_1(y_0)} + (a-1) + \frac{P}{S_1} \tag{33}$$

where $a$ is the same as in eq. 22.

The dependencies (31)-(33) are shown in Fig. 15 (dotted lines) for separation of $Cs^+$ - $Rb^+$ binary mixture on sulfo-phenolic resin. The different mutual positions of $\gamma$ limits (see Figs.15a-15c) depend on the equilibrium parameters of ion exchange system and on the value of product withdrawal,

TABLE 3. ASYMPTOTIC SITUATIONS IN TWO-SECTIONAL SEPARATION COLUMN

| No. | Section 1 | | Section 2 | |
|---|---|---|---|---|
| | Equilibrium is achieved in | Equilibration condition | Equilibrium is achieved in | Equilibration conditions |
| a | bottom | (26) | bottom | (28) |
| b | bottom | (26) | top | (27) |
| c | intermediate | (29) | top | (27) |
| d | top | (25) | top | (27) |
| e | intermediate | (29) | bottom | (28) |
| f | top | (25) | bottom | (28) |

$P/S_1$,. Letters "a,...,f" in Fig.15 denote $\gamma$ intervals corresponding to the respective situations in Table 3. Note that curve (31) can intersect curves (32) and (33), however their mutual location is always reduced to one of the cases shown in Fig.15.

Assuming that asymptotic equilibration of phases occurs in the same parts of sections, the balance equation (23) can be rewritten for situations "a-f" (see Table 3) in the form of the following six relations:

$$\gamma = a\frac{f_2(x_0)}{x_0 - x_P} - (a-1)\frac{x_P}{x_0 - x_P} - \frac{f_1(x_P)}{x_0 - x_P} \tag{34a}$$

$$a[f_2(x_P) - x_P] = f_1(x_P) - x_P \tag{34b}$$

$$\gamma = \left.\frac{df_1(x)}{dx}\right|_{x=x_1} + (a-1) + \frac{P}{S_1} = \frac{f_1(x_1)}{x_1 - x_P} - a\frac{f_2(x_P)}{x_1 - x_P} + (a-1)\frac{x_1}{x_1 - x_P} + \frac{P}{S_1} \tag{34c}$$

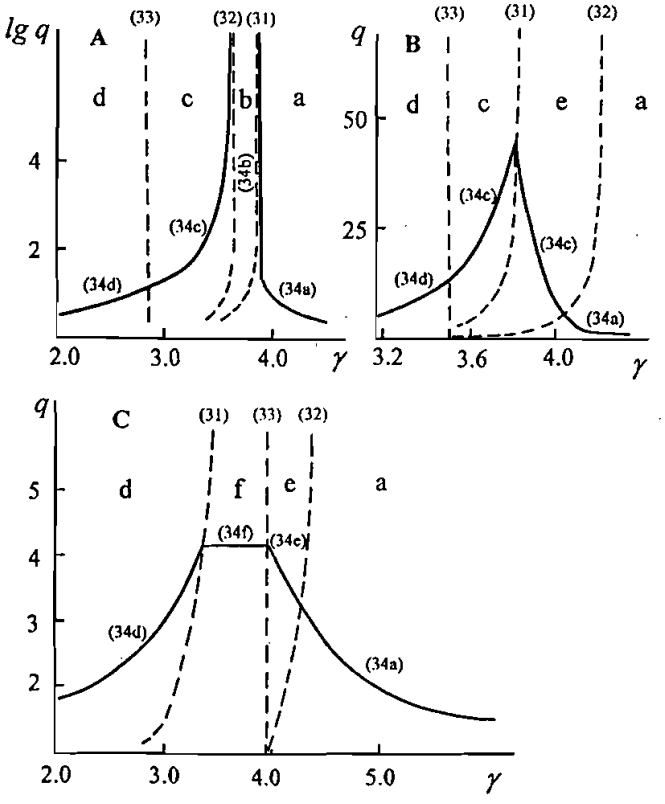


FIGURE 15. Asymptotic $q$ versus $\gamma$ dependencies for different $P/S_1$ values at $\alpha_1 = 1.64$; $\alpha_2 = 1.80$; $a = 3.0$; $x_0 - g_1(y_0) = 0.5$; $P/S_1 = 0$ (A); 0.56 (B); 1.0 (C) (see text).

$$\gamma = \frac{y_0}{g_1(y_0) - x_P} - a\frac{f_2(x_P)}{g_1(y_0) - x_P} + (a-1)\frac{g_1(y_0)}{g_1(y_0) - x_P} + \frac{P}{S_1} \tag{34d}$$

$$\gamma = \left.\frac{df_1(x)}{dx}\right|_{x=x_1} + (a-1) + \frac{P}{S_1} = a\frac{f_2(x_0)}{x_0 - x_1} -$$

$$-\frac{f_1(x_1)}{x_0 - x_1} - (a-1)\frac{x_1}{x_0 - x_1} - \frac{P}{S_1}\cdot\frac{x_1 - x_P}{x_0 - x_1} \tag{34e}$$

$$\gamma[x_0 - g_1(y_0)] = af_2(x_0) - (a-1)g_1(y_0) - y_0 - \frac{P}{S_1}[g_1(y_0) - x_P] \qquad (34f)$$

These equations define the asymptotic dependencies of the degree of separation $q \equiv \frac{1-x_P}{x_P} \Big/ \frac{1-x_0}{x_0}$ as a function of $\gamma$ for a dual-parametric column of infinite length at given equilibrium parameters of the system. Fig.15 shows the calculated (from the respective experimental data) $q$ vs $\gamma$ dependencies for separation of $Cs^+$ - $Rb^+$ on sulfo-phenolic resin KU-1 and the regions of their application. As seen, for three selected $P/S_1$ values the shapes of curves and the degrees of separation are very different due to the different mutual positions of the respective boundaries defined by equations (31) - (33).

Fig.16 shows the asymptotic $q$ versus $\gamma$ dependencies for separation of $K^+$ - $Na^+$ mixture on KU-1 resin at $P/S_1=0$. As seen, the separation by the "combine scheme" is not effective in this case due to the counter influence of two separation factors (see above).

At $a = 1$ the relations (34a)-(34f) transfer to the respective asymptotic relations corresponding to the "pure" dual-parametric separation process without flow reversal. The comparison of asymptotic relations obtained for the linear equilibrium dependencies $y = a_i x$ with the analytical solution (20) shows that only four of six situations defined in Table 3, namely "a", "b", "d" and "f", can be realized. In this case for $x_0 = y_0/\alpha_1$ the asymptotic relations can be rewritten as follows:

$$x_P = \frac{a \cdot \alpha_2 - \gamma}{\alpha_1 + (a-1) - \gamma} x_0 \qquad (35a)$$

$$x_P = 0 \qquad (35b)$$

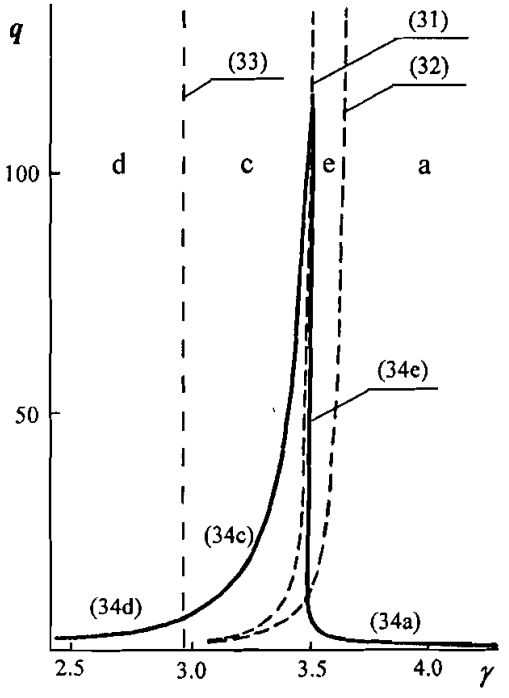


FIGURE 16. Asymptotic $q$ vs $\gamma$ dependencies for separation of $K^+$ and $Na^+$ on KU-1 resin (see text) at $\alpha_1 = 1.64$; $\alpha_2 = 1.40$; $a = 3.0$; $x_0 = g_1(y_0) = 0.5$ and $P/S_1 = 0$.

$$x_P = \frac{\alpha_1 + (a-1) + P/S_1 - \gamma}{a\alpha_2 - \gamma + P/S_1} x_0 \tag{35d}$$

$$x_P = \frac{\alpha_1 + (a-1) + P/S_1 - a\alpha_2}{P/S_1} x_0 \tag{35f}$$

The boundaries of $\gamma$ intervals, where these situations are realized, can be determined from equations $\gamma = a \cdot \alpha_2$ and $\gamma = \alpha_1 + (a-1) + P/S_1$.

Equation (35a) is also obtained from (20) at $N_1 \to \infty$ and $N_2 \to \infty$ if either $\gamma > a\alpha_2 > \alpha_1 + (a-1) + P/S_1$ or $\gamma > \alpha_1 + (a-1) + P/S_1 > a\alpha_2$ are valid. Similarly at $\gamma < \alpha_1 + (a-1) + P/S_1 < a\alpha_2$ or at $\gamma < a\alpha_2 < \alpha_1 + (a-1) + P/S_1$ one obtains (35d), and at $\alpha_1 + (a-1) + P/S_1 < \gamma < a\alpha_2$ or at $a\alpha_2 < \gamma < \alpha_1 + (a-1) + P/S_1$ from (20) we obtain (35b) and (35f), respectively. Hence, the asymptotic solutions of equation (20) giving relations (35a), (35b), (35d) and (35f) confirm the validity of these relations.

For a column of finite length, the $q$ vs $\gamma$ dependencies (calculated from eq. 20) appear to be located below the asymptotic ones (calculated from relations 35a-35f) and approach them when the numbers of transfer units in sections ($N_1$ and $N_2$) increases, as it is shown in Fig.17. The experimentally obtained $q$ vs $\gamma$ dependencies for separation of $Cs^+$- $Rb^+$, and $K^+$- $Na^+$ mixtures (see below) were also located inside $\gamma$ intervals determined by the asymptotic relations.

Fig.18 shows the asymptotic $q$ vs $\gamma$ dependencies for separation of $Rb^+$ from $Cs^+$ on KU-1 resin. As seen, the shapes of asymmetric curves change dramatically with variation of $P/S_1$. At small $P/S_1$ values, a certain interval of $\gamma$ values exists when $x_p = 0$ (i.e., when the completely purified rubidium is obtained), while as $P/S_1$ increases, this interval narrows. When the $P/S_1$ value exceeds a certain limiting value, the condition $x_p = 0$ cannot be fulfilled. The further increase of $P/S_1$ leads to the fast decrease of the maximal $q$ value. For high $P/S_1$ values the $q$ vs $\gamma$ dependence is characterized by the linearity region. Its slope is determined by the difference in composition of phases entering the column so that, e.g. at $x_0 = g_1(y_0)$ this slope is equal to zero. With the increase of $P/S_1$, the height of this region decreases while its width increases.

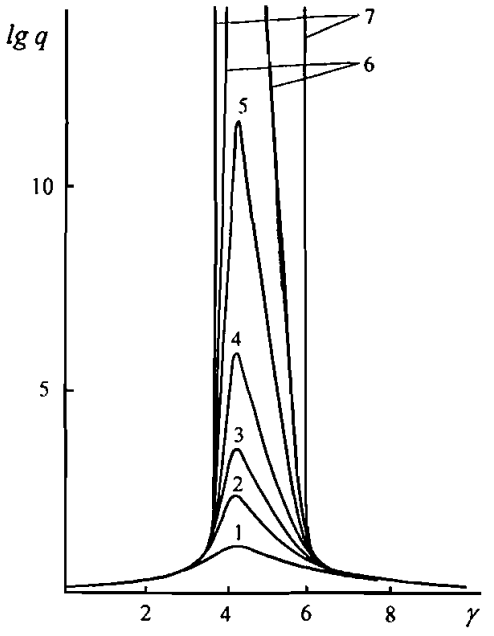


FIGURE 17. $q = x_0/x_P$ versus $\gamma$ plots for linear equilibrium dependencies $y=\alpha_i x$ at $\alpha_1 = 1.70$; $\alpha_2 = 1.96$; $a = 3.0$; $x_0 = 0.1$; $P/S = 0$, calculated by eq. (20) at $N_1 = N_2 = 5$ (1); 10 (2); 15 (3); 25 (4); 50 (5), and 100 (6); (7) correspond to asymptotic dependence.

The numerical analysis of the purification of rubidium from cesium on sulfo-phenolic resin, using solution (20) was carried out in [82; 84]. The experimental conditions under consideration (stock solutions) corresponded to either 0.3 N alkalis and 0.2 N salts mixture or 0.2 N solution of salts without alkalis. The equivalent fraction of cesium in all cases was $x_0 = 0.1$. The following experimental values of equilibrium parameters were used in calculations: $\alpha_2$=1.96; $\alpha_1$=1.70 and $a$=3.0. The main results obtained are shown in Figs. 19-23. The results of variation of $N_1$ values show (see Fig.19) that the decrease of $N_2$ (in alkaline zone) and $N_1$ (in neutral zone) results in a

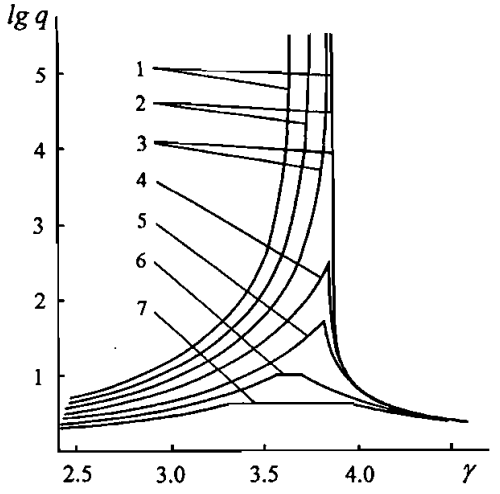


FIGURE 18. Asymptotic $q$ versus $\gamma$ dependencies for nonlinear isotherm $y = f(x)$ at $\alpha_1 = 1.64$; $\alpha_2 = 1.80$; $a = 3.0$; $x_0 = g_1(y_0) = 0.5$; $P/S = 0$ (1); 0.1 (2); 0.2 (3); 0.35 (4); 0.56 (5); 0.75 (6); 1.0 (7).

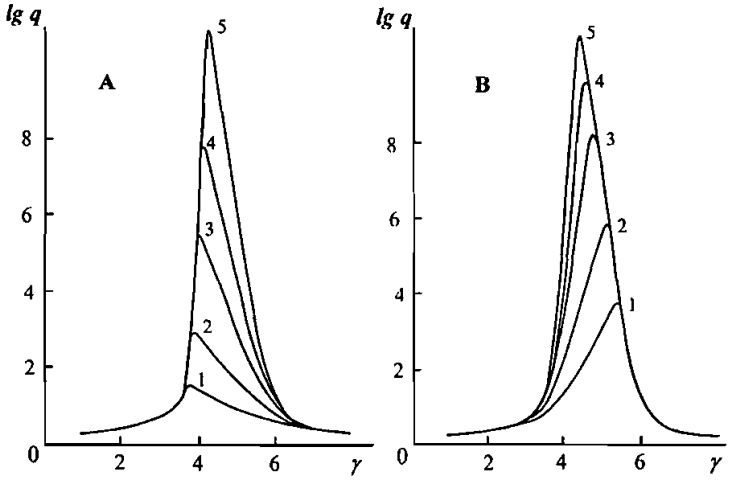


FIGURE 19. $q$ vs $\gamma$ plots calculated by eq. (20) at $\alpha_1 = 1.70$; $\alpha_2 = 1.96$; $a = 3.0$; $x_0 = 0.1$; $P/S = 0$. (A) $N_1 = 46$; $N_2 = 5$ (1); 10 (2); 20 (3); 30 (4); 46 (5), (B) $N_2 = 46$; $N_1 = 5$ (1); 10 (2); 20 (3); 30 (4); 46 (5).

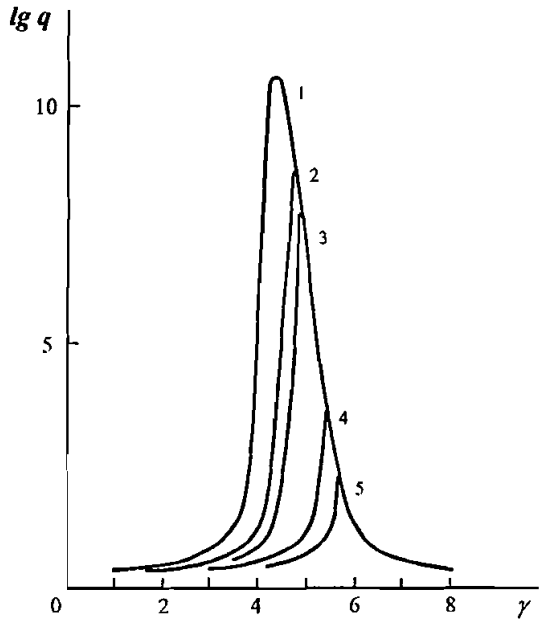


FIGURE 20. $q$ versus $\gamma$ plots calculated by eq. (20) at $\alpha_1$ = 1.70; $\alpha_2$ = 1.96; $a$=3.0; $x_0$ = 0.1; $N_1 = N_2$ = 46; $P/S$ = 0 (1); 0.5 (2); 0.75 (3); 1.5 (4); 2.0 (5).

significant decrease of the degree of separation. At the same time, $\gamma_{opt}$ shifts to lower values in the first case and to higher values in the second. An increase of product withdrawal $P/S_1$ (see Fig. 20) leads to a decrease in $q_{max}$ and to the narrowing the flows ratio interval $\gamma$. The position of $\gamma_{opt}$ is shifted to the range of higher values.

The results of these calculation show significant influence of the flow reversal degree, $a = S_2 / S_1$ on the efficiency of CPS. The comparison of curves 2-5 with curve 1 in Fig.21 illustrates much higher efficiency of CPS in comparison with the simple dual-parametric process. As seen, the increase of $a$ value leads to the growth of separation degree $q$, and to the

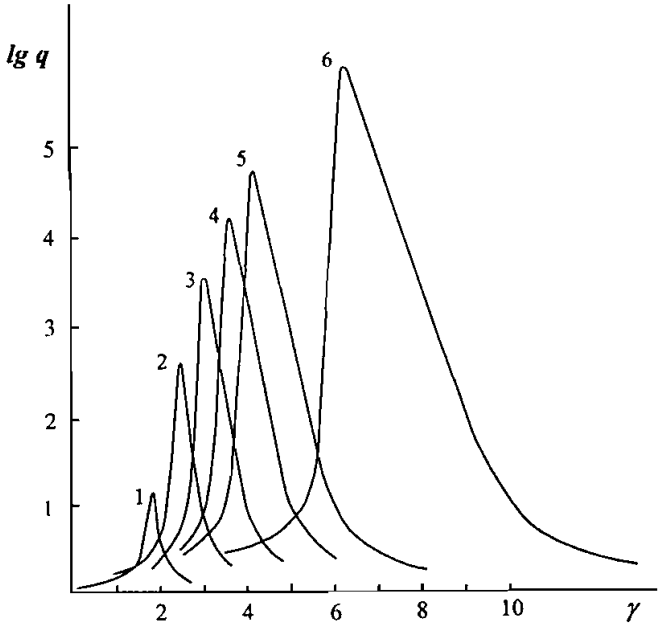


FIGURE 21. $q$ versus $\gamma$ plots calculated by eq. (20) at $\alpha_1$ = 1.70; $\alpha_2$ = 1.96; $x_0$=0.1; $N_1 = N_2 = 20$; $P/S = 0$; $a$ = 1.0 (1); 1.5 (2); 2.0 (3); 2.5 (4); 3.0 (5); 5.0 (6).

widening of $\gamma$ interval. The increase of equilibrium separation coefficient $\alpha_2$ and the decrease of $\alpha_1$ also result in a significant increase of $q_{max}$ and in expansion of $\gamma$ interval (see Fig.22).

Both in a simple dual-parametric separation (see Fig.10) and in CSP at $\gamma < \gamma_{opt}$ the purified component is accumulated in the bottom section. At $\gamma > \gamma_{opt}$ the product is accumulated in the top section, while at $\gamma = \gamma_{opt}$ the symmetric distribution of $q$ vs $z$ is observed (see Fig.23).

To conclude this section we would like to emphasize that the efficiency of CSP depends on the following parameters:

(1) the variation of ion-exchanger capacity at the boundary between sections with neutral and alkaline solutions;

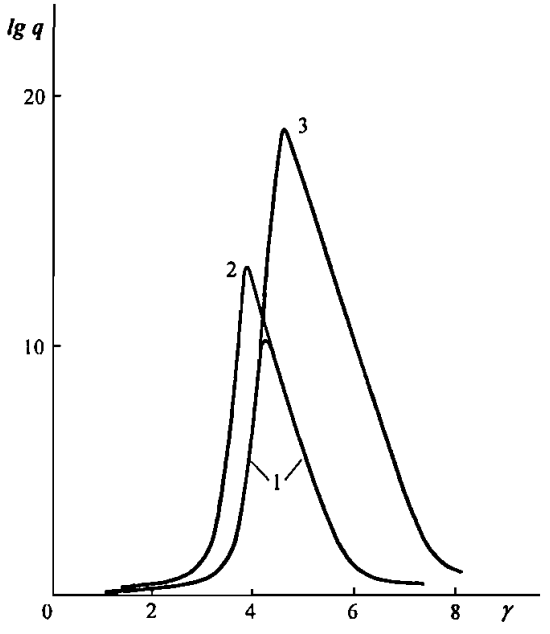


FIGURE 22. $q$ versus $\gamma$ plots calculated by eq. (20) at $N_1 = N_2 = 46$; $a$=3.0; $x_0$ = 0.1; $P/S = 0$ and $\alpha_1$ and $\alpha_2$ = 1.70 and 1.96 (1); 1.20 and 1.96 (2); 1.70 and 2.50 (3).

(2) the difference in equilibrium separation coefficients in column sections; (3) the ratio of the mixture flows entering the column with solution and ion exchanger phases. This ratio depends either on the ratio of alkalis to salts in solution in concentrating the weaker sorbed component or on the ratio of acid to salts in the opposite case (concentration of a stronger sorbed component).

## 5c. Non-Steady-State Dual-Parametric and CPS

The theory of non-steady-state dual-parametric and CSP is practically undeveloped so far. A brief review of some work in this field is given below.

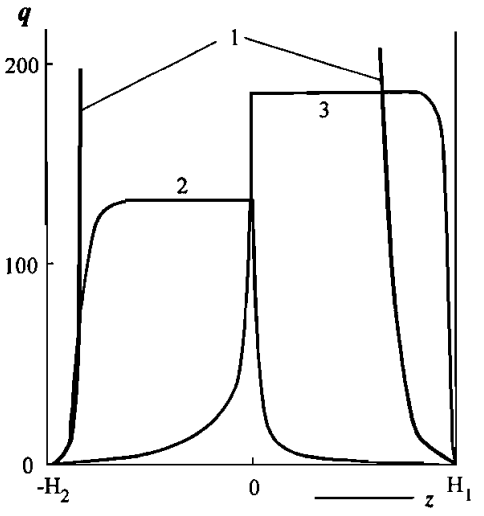


FIGURE 23. $q$ versus $z$ calculated by eq. (20) at $\alpha_1 = 1.70$; $\alpha_2 = 1.96$; $x_0 = 0.1$; $a$=3.0; $N_1 = N_2 = 46$; $P/S = 0$ and different values of flows ratio: (1) $\gamma_{opt}$= 4.24; (2) 3.71; (3) 5.70.

The results of the first investigations of a large-scale dual-temperature separation of hydrogen isotopes by chemical exchange at linear equilibrium dependence were published in monographs [65, Part 11.7; 72, Part 3.7]. The approach applied was based on the following assumptions: 1) the equivalence of non-stationary mass-transport of the component in column and external steady-state withdrawal of the product, and 2) the time dependencies of product concentration for different coordinates along the column were similar.

In [85] the authors showed the inadequacy of these assumptions. They solved the task of separation in dual-parametric column using an original quasi-homogenous mathematical model analogous to the equilibrium diffusional model supposing the fast equilibration of phases and

axial dispersion. The authors obtained the expression describing separation at a very initial period of column operation.

Later, the kinetics of concentration of the microcomponent in CSP was analyzed in a more general form [80] using the equilibrium diffusional model. It was shown that the optimal conditions for the starting period of the column operation could significantly differ from that for the steady-state operation.

The time evolution of dual-temperature separation and that of CSP at nonlinear equilibrium dependence were investigated in [30] and [86], respectively. The equilibrium model of plug flow was used in both of these works. The different types of evolution and concentration profiles in sections as well as the intervals of corresponding flows ratio were examined. Expressions for the maximal concentration in system for the whole range of variations of controlling parameters were obtained.

### 5d. Separation in Fixed Bed Column with Moving Boundary of Zones

One important feature of the processes based on pH variations (see Fig.11), which allows carrying out the CSP in the fixed bed columns must be emphasized. When the sorption front dividing the alkaline and neutral or acidic and alkaline zones moves along the column, the border between sections 1 and 2 moves as well. In this case, the separation process is governed by the ratio of flows through the moving boundary between zones.

When the mixture of alkalis and salts of the separated ions is passed through the column with sulfo-phenolic resin pre-equilibrated with the same salts mixture (see flow-sheet in Fig.11a), the flows through this boundary can be expressed as follows:

$$L_2 = \chi(v-u)c'' \tag{36}$$

$$S_1 = (1-\chi)(u-w)m' \tag{37}$$

Here $u$ is the rate of the boundary (the sorption front) movement; $v$ and $w$ are the actual linear flow rates of solution and ion exchanger, respectively, related to the column walls ($v > 0$, $w < 0$); $c'$ and $c''$ are the total concentrations of ions to be separated in neutral (or acidic) and in alkaline solutions, respectively; $m'$ and $m''$ are the total concentrations of ions to be separated in the ion exchanger equilibrated with solution of concentrations $c'$ and $c''$; $\chi$ is the fractional void volume of the resin bed ($\chi$, $v$ and $w$ are assumed to be constant along the column).

The rate of the steady-state front movement is defined by the following expression [87]:

$$u = \frac{\chi\ v(c''-c') + (1-\chi)w(m''-m')}{\chi(c''-c') + (1-\chi)(m''-m')} \tag{38}$$

From equations (36)-(38) one obtains:

$$\frac{L_2}{S_1} = \frac{c''(m''-m')}{m'(c''-c')} = \frac{(a-1)}{\left(1-\frac{c'}{c''}\right)} \tag{39}$$

The last equation shows that the flows ratio depends on $c'/c''$ only when $a \equiv m''/m'$ is constant. The $a$ value depends on the concentration of alkalis in solution, and $c'/c''$ ratio is determined by the ratio of salts and alkalis concentration in the initial solution. Equation (39) is also valid for a fixed bed column, i.e. when $w$=0.

Fig.24 shows one of the breakthrough curves obtained by passing the mixture of cesium and rubidium salts and alkalis ($c_{Cs}$:$c_{Rb}$ =1, $c_{OH}$ = 0.315

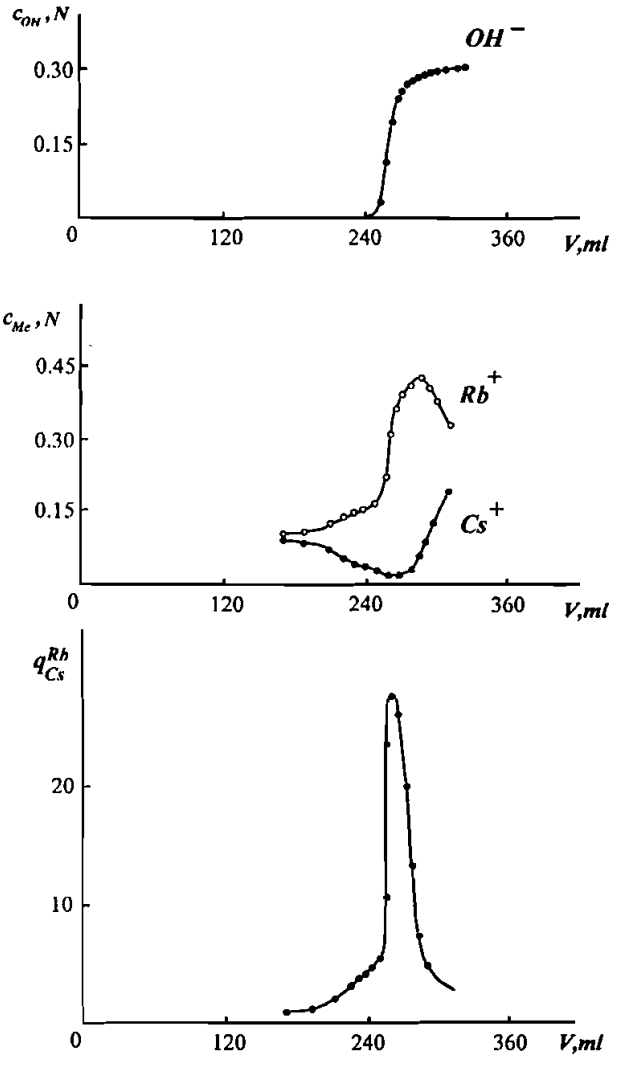


FIGURE 24. Concentration-volume histories for $OH^-$ (A), and $Cs^+$ and $Rb^+$ (B), and separation degree, $q_{Cs}^{Rb} = \frac{1 - x_{max}}{x_{max}} \Big/ \frac{1 - x_0}{x_0}$, versus volume plot (C). Conditions: initial solution: 0.316 equiv/l MeOH + 0.207 equiv/l $MeNO_3$ ($x_{Cs}$ = 0.5); sulfo-phenolic resin KU-1; height of resin bed = 70 cm; solution flow-rate = 1.2 ml/min [28; 88].

N, $c''$ = 0.522 N) the fixed bed column with sulfo-phenolic cation exchanger KU-1 (with bead size of 0.08-0.25 mm) pre-equilibrated with 0.21 N solution of cesium and rubidium nitrates (1:1) [28; 88]. The sorption of cesium and rubidium on phenolic groups of ion exchanger is accompanied by a change in ratio of the mixture components at the boundary between alkaline and neutral zones. Note, that *the dual-parametric fractionation on a fixed bed of bi-functional ion exchanger can be considered as a new chromatographic separation technique.*

From the experimental breakthrough curves one can obtain all necessary data for calculation of the flows ratio. Indeed, it is easy to show that:

$$(c''-c')(V-V_0) = Q'(a-1) \tag{40}$$

where $V$ is the volume of solution passed through the column until the appearance of the midpoint of sorption front; $V_0$ is the void volume of the column prior the start of experiment, and $Q'$ is the amount of the mixture been sorbed by the resin bed before the experiment. Note that $Q'$ value can be a bit less than the ion-exchange capacity of the resin by the sulfonic groups only (see below).

Equations (39) and (40) give the following expression for calculation of the flows ratio from respective experimental data:

$$\frac{L_2}{S_1} = \frac{c''(V-V_0)}{Q'} \tag{41}$$

The results of experiments with different ratio of concentrations of salts and of alkalis is shown in Fig. 25, where the dependence of maximal separation degree, $q_{Cs}^{Rb}$, on the flows ratio is presented [28; 88].

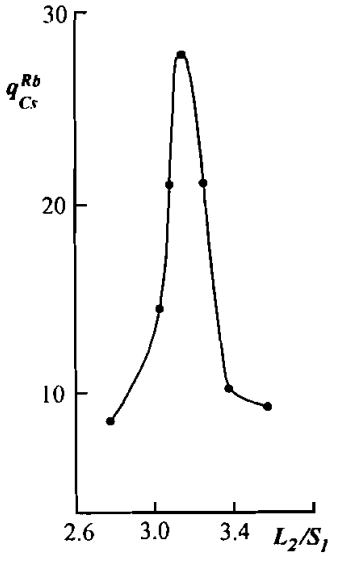


FIGURE 25. $q_{max}$ versus flows ratio plot for concentration of $Rb^+$ on KU-1 resin. Conditions: identical to those in Fig. 24 [28; 88].

Concentration of salts in the initial alkaline solution was varied from 0.13 to 0.30 N, while the concentration of alkalis was kept constant at 0.32 N level. As seen in Fig. 25, the maximum on $q_{Cs}^{Rb}$ curve corresponds to $L_2/S_1 \approx 3.1$. This value did not change with the increase of the resin bed height, despite the growth of $q_{max}$. The comparison of experimentally determined optimal flows ratio with that estimated from the asymptotic dependencies (see Fig.18) for the same system shows that the experimental value of $\gamma_{opt.}$ is a bit less than the calculated one. However, this deviations decreases as the initial fraction (in stock solution) of the component under concentration (rubidium) increases (see below Table 4).

In experiments carried out at $\gamma =. \gamma_{opt.}$ , the maximal separation degree was achieved in the eluate fractions corresponding to the midpoint of

the sorption front. In experiments with $\gamma > \gamma_{opt}$, the maximal separation shifted to the initial part of sorption front (corresponding to the neutral zone), and at $\gamma < \gamma_{opt}$, the maximal separation displaced to the alkaline zone.

When passing the acidified mixture of salts through the column (within the same series of experiments described above) a stronger sorbed component (cesium) is concentrated. Fig. 26 shows one of the breakthrough curves obtained with solution containing 0.22 N equi-molar mixture of $CsNO_3$ and $RbNO_3$ and 2.45 N acetic acid [28; 88]. The experiment described represents a fixed bed version of CSP shown in Fig.11b. In this case the separation efficiency depends on the flows ratio as follows:

$$\frac{L_1}{S_2} = \frac{\chi\ c'(v-u)}{(1-\chi)m''(u-w)} \tag{42}$$

The velocity of the steady-state front movement along the resin bed, $u$, can be expressed through the concentrations of ions to be separated and the concentration of acid, $c_a$, as follows:

$$u = \frac{\chi\ vc_a + (1-\chi)wm_a}{\chi c_a + (1-\chi)m_a} \tag{43}$$

where $m_a$ is the amount of acid reacting with a unit volume of ion exchanger (or the concentration of that part of the resin functional groups which changes the ionic form when interacting with acidic solution).

Equations (42) and (43) yield

$$\frac{L_1}{S_2} = \frac{c'm_a}{cm''} \tag{44}$$

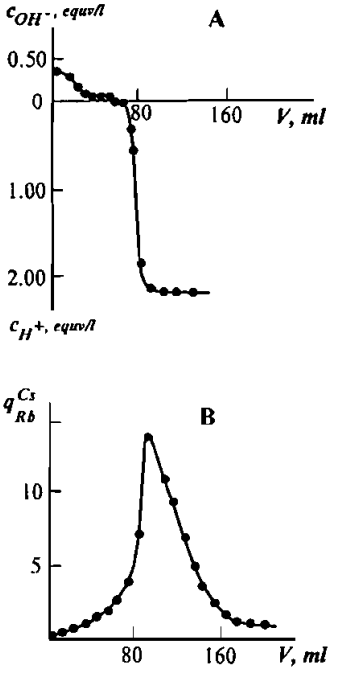


FIGURE 26. Concentration-volume histories for $OH^-$ and $H^+$ (A), and separation degree $q_{Rb}^{Cs} = \frac{x_{max}}{1-x_{max}} / \frac{x_0}{1-x_0}$ versus volume dependence(B) for concentration of $Cs^+$ on KU-1 resin from stock solution of 0.22 equiv/l $MeNO_3$ + 2.45 equiv/l $CH_3COOH$ ($x_{Cs}$ = 0.5). Conditions: identical to those in Fig. 24 [28; 88].

The ratio $m_a/m''$ can be determined in the fixed bed separation experiments from the amount of acid passed through the column until the appearance of midpoint of the sorption front:

$$\frac{m_a}{m''} = \frac{(V - V_0) \cdot c_a}{Q' \cdot a} \tag{45}$$

where $Q'$ is the amount of ions mixture remaining in the ion exchanger after its contact with acidic solution. Finally, we obtain

$$\frac{L_1}{S_2} = \frac{(V - V_0) \cdot c'}{Q' \cdot a} \tag{46}$$

Parameter $a$ characterizes the difference of flows of the separating ions with an ion exchanger in different zones of column. Value of $a$ can be estimated from the equilibrium data [17] for the sulfo-phenolic resin as the ratio of its sorption capacity by both phenolic and sulfonic groups (determined in alkali solution of a given concentration) to the capacity of the same resin by sulfonic groups only (in neutral solution). The value of $a$ depends on the concentration of alkali and practically does not depend on the nature of cation. For example, for KU-1 resin it has been found $a$=2 at $c_{OH}$=0.01 N and this parameter increases to $a \approx 3$ at $c_{OH}$=0.2-0.3N [17].

The value of $a$ determined in experiments with acidic solutions (see above), can differ from that determined from the equilibrium data due to the partial displacement of cations from sulfonic groups by protons. More precisely the $a$ value can be found directly from the results of separation experiment using the following relation:

$$a = \frac{(V - V_0)(c'' - c')}{Q'} + 1 \tag{47}$$

The results of three experiments on concentration of cesium in the fixed bed column are presented in Fig. 27. In the first run carried out at $c'$=0.22 N, the concentration of acetic acid was varied. In the second run, the acid concentration was kept constant at $c_{H+}$=0.82 N level, while the concentration of salts was varied keeping constant the ionic ratio of cesium to rubidium. In the third run the hydrochloric acid was used to acidify the initial solution. In all three experiments the optimal values of $(L_1/S_2)_{opt}$ were found to be the same. The effectiveness of the separation process increased

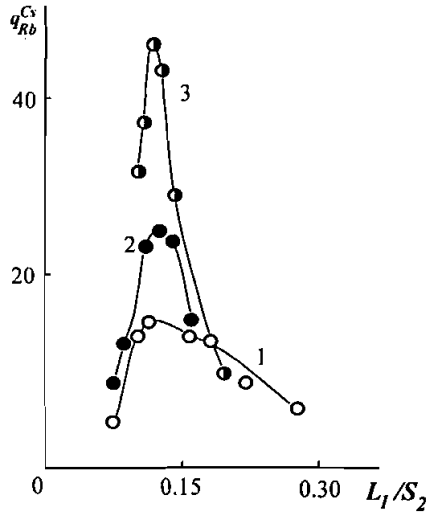


FIGURE 27. Maximal separation degree $q_{Rb}^{Cs}$ versus $L_1/S_2$ plots obtained in three experiments with fixed bed of KU-1 resin (see text). (1) $c'$ = 0.22 N = const., concentration of $CH_3COOH$ was varied; (2) $c_{H^+}$ = 0.082 N = const. ($CH_3COOH$), $c'$ was varied; (3) $c'$ = 0.22 N = const., concentration of HCl was constant (1.0 N) and concentration of $CH_3COOH$ was varied [28; 88].

significantly when salts solution was acidified with HCl instead of acetic acid. Indeed, a stronger acid (HCl) displaced more separated ions from sulfonic groups that resulted in the increase of $a$ value.

The results obtained by purification of $Rb^+$ from $Cs^+$ ($x_{Cs}$=0.1) and $Cs^+$ from $Rb^+$ ($x_{Rb}$=0.1) are collected in Table 4 [84]. These results indicate to the high efficiency of the process. Note, that both in fixed bed and in counter-current versions of the process, the regeneration of ion exchanger is not required.

## 5e. Optimization of Flows Ratio

The main problem in the practical use of dual-parametric and CSP is the determination of the optimal flows ratio. To solve this problem, one

TABLE 4. PURIFICATION OF $Rb^+$ FROM $Cs^+$ AND OF $Cs^+$ FROM $Rb^+$
(column height = 28 cm; i.d. = 0.8 cm; solution flow rate = 1.4 cm/min)

| Purification of $Rb^+$ from $Cs^+$ $X_{Cs}$=0.1, [MeOH]=0.300 N | | | Purification of $Cs^+$ from $Rb^+$ $x_{Cs}$=0.9, [$MeNO_3$]=0.100 N | | |
|---|---|---|---|---|---|
| [$MeNO_3$], N* | $L_2/S_1$ | $q_{max}$ | [$CH_3COOH$], N* | $L_1/S_2$ | $q_{max}$ |
| 0.237 | 3.46 | 14 | 1.400 | 0.069 | 19 |
| 0.382 | 4,18 | 96 | 0.750 | 0.106 | 130 |
| 0.423 | 4.72 | 133 | 0.604 | 0.134 | >400 |
| 0.450 | 4.90 | 172 | 0.445 | 0.162 | >400 |
| 0.526 | 5.39 | 121 | 0.202 | 0.31 | 4 |
| 0.637 | 6.24 | 14 | | | |

- in the initial solution.

needs to know the following parameters of the system [89, 90]: 1) equilibrium dependencies $y=f_1(x)$ and $y=f_2(x)$ under conditions in both sections of column; 2) the ratio of the specific capacities of the resin (mg-equiv/g) under conditions in sections; and 3) the numbers of transfer units in sections. The optimization of separation process includes the following steps:

1. The theoretical estimation of the favorable interval of flows ratio using either asymptotic relations (34a) - (34f) (or 35a, 35b, 35d and 35f) or the analytical solutions of (20) type. In any case, the theoretical estimation obtained in this step or from the results of the further experiments must be corrected during the operation of the separation set-up.

2. Determination of the optimal flows ratio in a set of experiments on a fixed bed column (if possible).

3. Test-experiments on the separation counter-current column using the flow-ratio estimated either in step 1 or in step 2 and simultaneous

correction of the flows ratio based on the character of distribution of the accumulated component along the column.

This optimization scheme was used in the process of purification of $Rb^+$ from $Cs^+$ ($x_{0,Cs}$=0.1) on KU-1 resin. The estimations obtained by the asymptotic relations (35a), (35b), (35d) and (35f) gave the favorable flows-ratio interval $L_2/S_1$≈3.7-6.0 (see Fig.17). The calculations made have shown also that this interval narrows and shifts to the lower boundary when operating with the product withdrawal.

The calculations by the analytical solution (20) carried out for equal $N_i$ values in sections gave the optimal $L_2/S_1 \approx 4.3$ (see Fig.17). The optimal flows ratio determined in a set of experiments on the fixed bed column (see Table 4) appeared to be $L_2/S_1$= 4.9±0.1, i.e. it was a bit higher than that calculated by (20).

These estimates were used in the purification process on the counter-current column (column height = 2.2 m; i. d. = 2.6 cm; continuous movement of ion exchanger from the top to bottom with counter-flow of solution). First, the separation column was operating at $L_2/S_1$= 4.9. The feeding solution represented the mixture of alkalis (0.300 N) and salts (0.455 N) of rubidium and cesium with $x_{Cs}$=0.1. The KU-1 resin was pre-equilibrated with the mixture of RbCl and CsCl with $x_{Cs}$=0.1. The flow-rates of phases were kept so that the boundary between alkaline and neutral zones in column was stationary and located near the middle point of the column. Under these conditions (see Fig.28a) the rubidium enriched zone was formed rather fast, however, it was shifted to the upper part of the column. As the result, a significant loss of the partly purified $Rb^+$ with solution leaving the column was observed even in the initial period of column operation. These facts indicated that the operating flows ratio exceeded the optimal value.

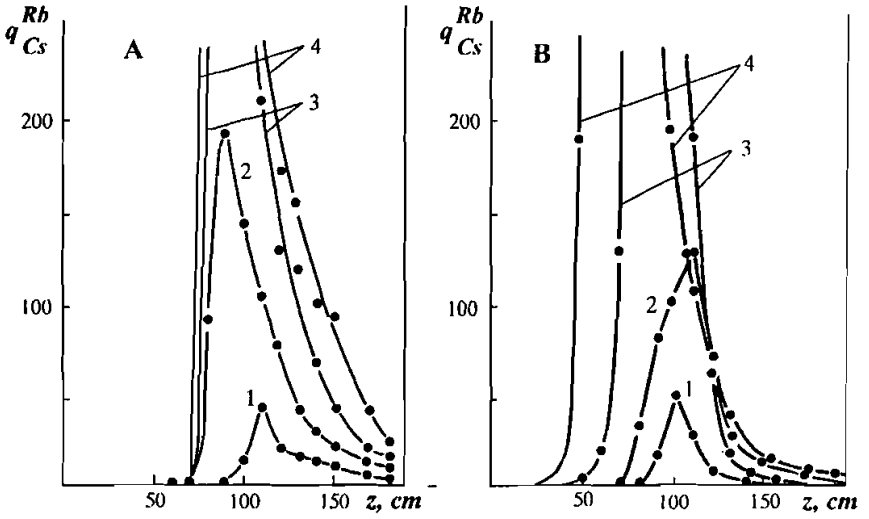


FIGURE 28. Plots of separation degree $q_{Cs}^{Rb}$ versus coordinate along counter-current column ($z$) in experiments with different flows ratio, $L_2/S_1$. (A) $L_2/S_1$=4.9; operation time, t, (hrs): (1) 28; (2) 43; (3) 54 and (4) 66.(B) $L_2/S_1$=4.0; t = (1) 17; (2) 33; (3) 57 and (4) 69 (see text) [89; 90].

Then, based on the results of modeling analysis, the flows ratio was diminished to $L_2/S_1$= 4.0. For this, the concentration of salts in the initial solution was decreased to 0.350 N at the same concentration of alkalis 0.300 N. As the result, the $q$ vs $z$ dependencies became more symmetrical, and the loss of the purified rubidium at the column edges remarkably decreased (see Fig.28b). The solution of purified $Rb^+$ with $Cs^+$ content decreased by a factor > $10^3$ was collected from the middle part of the column.

A similar procedure was used for optimization of separation of cesium from rubidium [88]. Experimental results are shown in Fig.29. The process was carried out in the column with the counter-flow of phases similar to the well-known Higgins' contactor [91]. The dynamic properties

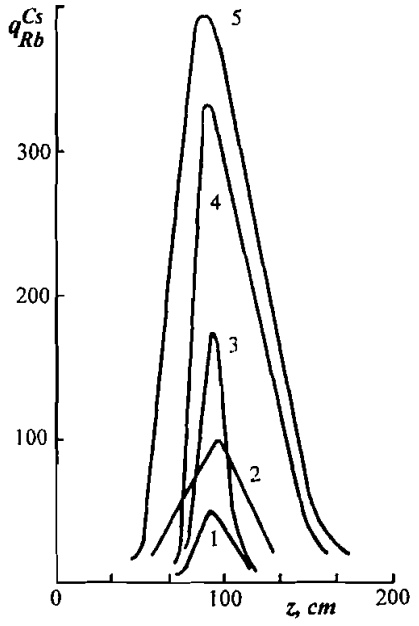


FIGURE 29. Plots of separation degree $q_{Rb}^{Cs}$ versus coordinate along counter-current column ($z$). Conditions: initial solution: 0.207 mol/l $RbNO_3$+ $CsNO_3$ (1:1) + 2.25 mol/l $CH_3COOH$; $v$ = 87 cm/hr; $w$ = 27 cm/hr; operation time, (hrs): (1) 4; (2) 8; (3) 19; (4) 20 and (5) 21.

of the experimental set-up are described in [92]. More detailed experimental results on separation of cesium and rubidium (and sodium and potassium as well) are given in [78, 88, 89, 93].

## LIST OF SYMBOLS

$a = S_2/S_1$ - the ratio of ion flows with ion exchanger phase in different sections of column;

$c$ - the concentration in solution phase, equiv/l;

$F = S_2 - S_1$ - the difference of ion flows with ion exchanger phase in different sections of column, equiv/cm$^2$ min;

$h$ - the height of transfer unit, cm;

$H$ - the height of column or section of column, cm;

$i$.- the number of stage;

$k$ - the mass transfer coefficient, equiv/cm$^3$ min;

$\tilde{K}$ - the equilibrium concentration constant;

$K$- the selectivity coefficient;

$L$ - the density of solution flow, equiv/cm$^2$ min;

$m$ - the concentration in resin phase, equiv/l;

$N$ - the number of transfer units;

$P$ - the flow density of product withdrawal, equiv/cm$^2$ min;

$Q$ - the amount of ions mixture in the resin phase, equiv;

$q$ - the degree of separation;

$S$ - the density of resin flow, equiv/cm$^2$ min;

$u$ - the velocity of movement of sorption front along the resin bed, cm/min;

$V$ - the volume of solution, ml;

$v$ - the linear solution flow rate in column, cm/min;

$w$ - the linear resin flow rate in column, cm/min;

$x$ - the equivalent fraction of ion in solution;

$y$ - the equivalent fraction of ion in resin;

$z$ - the coordinate along the column, cm;

$z_{A,B}$ - the charges of ions;

$\alpha$ - the equilibrium separation coefficient;

$\beta$ - the equilibrium enrichment coefficient;

$\chi$ - the fractional void volume of the resin bed;

$\Theta$ - the degree of flow cut in a single separation unit;

$\gamma = L/S$ - the ratio of flows with different phases in column;

$\varphi$ - the degree of purification.

## REFERENCES


1. F. Helfferich, Ion Exchange, McGraw-Hill, New York (1962).
2. J.D. Cosgrove and J.D.N. Strickland, J.Chem.Soc., 7, 1845 (1950).
3. P. Gregor and J. Bregman, J.Colloid.Sci., 6, 1614 (1951).
4. D. Dickel and A. Meyer, Z. Electrochem., 57, 901 (1953).
5. W.Rieman and H.Walton, Ion Exchange in Analytical Chemistry, Pergamon Press, New York (1970).
6. G. Klein, M. Villena-Blanco and T. Vermeulen, Ind. Eng. Chem. Process Des. and Develop., 3(3), 280 (1964).
7. K.M. Saldadze and E.A. Sheinina, in Chromatography, Theory and Application, Ed. K.V.Chmutov, Izd. AN SSSR, 1960, p.33 (Russian).
8. V.S. Soldatov, L.P. Novitskaya, M.S. Bespalko and Z.I. Kogan, in Synthesis and Properties of Ion Exchange Materials, K.V.Chmutov, Ed., Nauka, Moscow, 1968, p. 216 (Russian).
9. D.E. Weiss, B.A. Bolto, R. McNeill, A.S. Macpherson, R. Suidak, E.A. Swinton and D. Willis, Aust.J.Chem., 19 (5), 765; 791 (1966).
10. B.A. Bolto, R. McNeil, A.S. Macpherson, R. Suidak, D.E. Weiss and D. Willis, Aust. J. Chem., 21, 2703 (1968).
11. B.A. Bolto, R.J .Eldridge, K.H. Eppinger and M.B. Jackson, React. Polym., 2, 5 (1984).
12. V.D. Timofeevskaya, V.A. Ivanov and V.I. Gorshkov, Zh.Fiz.Khim., 62(9), 2531 (1988) (Russian). English translation in Russ.J.Phys.Chem., 62(9), 1314 (1988).
13. V.A. Ivanov, V.D. Timofeevskaya, V.I. Gorshkov and S.N. Grishenina,

Zh.Fiz. Khim., 63, 1867 (1989) (Russian). English translation in Russ.J.Phys.Chem., 63 (7), 1021 (1989).

14. V.A. Ivanov, V.D. Timofeevskaya, V.I. Gorshkov and T.V. Eliseeva, Zh. Fiz. Khim., 65, 2455 (1991) (Russian). English translation in Russ.J.Phys.Chem., 65 (9), 1296 (1991).
15. V.I. Gorshkov, M.V. Ivanova and A.M. Kurbanov, Zh.Fiz.Khim., 48, 1237 (1974) (Russian).
16. E.N. Gapon, Zh. Obshch. Khim., 3, 660 (1933) (Russian).
17. V.I. Gorshkov, M.V. Ivanova and V.A. Ivanov, Zh. Fiz. Khim. 51(8), 2084 (1977) (Russian).
18. V.A. Ivanov and V.I. Gorshkov, Zh. Fiz. Khim., 53(10), 2630 (1979) (Russian).
19. B. Tremillon, Les separations par les resines echangeuses d`ions, Gauther-Villars-Paris (1965).
20. K. Dorfman, in Ion Exchange Resins, K. Dorfman, Ed., Walter de Gruyter, Berlin, 1992, Ch. 1.2.
21. P.C. Wankat, in Percolation processes. Theory and Applications, A.E. Rodrigues and D.Tondeur, Eds., Sijthoff and Noordhoff Int. Publ., Rockville-Maryland, 1981, p.443.
22. G. Grevillot, in Handbook of Heat and Mass Transfer, Vol.2, Mass Transfer and Reactor Design, N.P. Cheremisinoff, Ed., Gulf Publ., Houston, 1986, p.1429.
23. D. Tondeur and G. Grevillot, in Ion Exchange Science and Technology, NATO ASI, Vol.107, A. Rodrigues, Ed., Martinus Nijhoff Publ., Dordrecht, 1986, p.369.
24. B.M. Andreev, G.K. Boreskov and S.G. Katal'nikov, Khim. Prom., 6, 389 (1961) (Russian).

25. B.M. Andreev and G.K. Boreskov, Zh. Fiz. Khim., 38, 115 (1964) (Russian).

26. V.I. Gorshkov, A.M. Kurbanov and N.V. Apolonnik, Method for Separation of Substance Mixtures, Pat.USSR 348029 (1970).

27. V.I. Gorshkov, A.M. Kurbanov and N.V. Apolonnik, Zh. Fiz. Khim. 45, 2669 (1971) (Russian).

28. V.I. Gorshkov, M.V. Ivanova, A.M. Kurbanov and V.A. Ivanov, Vestn. Mosk. Univ., Khimiya, 18, 535 (1977) (Russian). English translation in Moskow University Chemistry Bulletin. 32, (5), 23 (1977).

29. M. Bailly and D. Tondeur, AIChE, Symp. Ser., 54, 111 (1978).

30. M. Bailly and D. Tondeur, J.Chromatogr., 201, 343 (1980).

31. D. Tondeur, in Percolation Processes. Theory and Applications, A.E. Rodrigues and D.Tondeur, Eds., Sijthoff and Noordhoff Int. Publ., Rockville-Maryland, 1981, p.517.

32. R. Kunin and R.J. Myers, Ion Exchange Resins, Wiley, New York (1950).

33. A.I. Vulikh, Ion Exchange Synthesis, Nauka, Moscow (1976) (Russian).

34. G.K. Feiziev, Highly Effective Methods for Softening, Desalination and Demineralization of Waters, Energoatomizdat, Moscow (1988) (Russian).

35. Shun-ichi Watari and Hiromu Hayashi, in Proc. Intern. Conf. on Ion Exchange ICIE.'95, General Education and Training Center (Shikoku Electric Power Co., Inc) Takamatsu, Japan, 1995, p.499.

36. V.A. Ivanov, V.D. Timofeevskaya, V.I. Gorshkov and T.V. Eliseeva, Visokochistye Veschestva, 4(2), 133 (1990) (Russian). English translation in High Purity Substances. 4, 309 (1991).

37. V.A. Ivanov, V.D. Timofeevskaya and V.I. Gorshkov, React. Polym., 17, 101 (1992).

38. V.A. Ivanov, V.I. Gorshkov, N.V. Drozdova, V.D. Timofeevskaya and I.V. Staina, Visokochisdtye Veschestva, 6, 13 (1996) (Russian).

39. V.A. Ivanov, V.D. Timofeevskaya, V.I. Gorshkov and N.V. Drozdova, J. Radioanal. and Nucl. Chem., 208, 23 (1996).

40. V.I. Gorshkov and M.S. Safonov, Zh. Fiz. Khim., 42(6), 1459 (1968) (Russian).

41. V.I. Gorshkov and M.S. Safonov, Zh. Fiz. Khim., 42 (6), 1466 (1968) (Russian).

42. D. Muraviev, J. Noguerol and M. Valiente, React. & Funct. Polym., 28, 111 (1996).

43. D. Muraviev, A. Gonzalo and M .Valiente, Anal. Chem., 67, 3028 (1995).

44. D. Muraviev, J. Noguerol and M. Valiente, Hydrometallurgy, 44, 331 (1997).

45. D. Muraviev, J. Noguerol and M. Valiente, in Progress in Ion Exchange. Advances and Applications, A. Dyer, M.J. Hudson and P.A. Williams, Eds., SCI, Cambridge, 1997, p. 349.

46. D. Muraviev, J. Noguerol and M. Valiente, Environ. Sci. Technol., 31, 379 (1997).

47. A.A. Zagorodny and M. Muhammed., in Progress in Ion Exchange. Advances and Applications, A.Dyer, M.J.Hudson and P.A.Williams, Eds., SCI, Cambridge, 1997, p. 383.

48. N.P. Nikolaev, D. Muraviev and M. Muhammed, Sep. Sci. Technol., 32(1-4), 849 (1997).

49. T.J. Butts, N.H. Sweed and A.A. Camero, Ind. Eng. Chem. Fundam., 12(4), 467 (1973).

50. T. Szanya, L. Hanak and R. Mohila, Zh. Prikl. Khim., 56(10), 2194 (1986) (Russian).

51. T. Szanya, L. Hanak and R. Mohila, Hung. J. Chem. Veszp., 16, 261 (1988).

52. G. Grevillot, I. Dodds and S. Marques, J. Chromatogr., 201, 329 (1980).

53. G. Grevillot and D. Tondeur, in Ion Exchange Technology, D.Naden and M.Streat, Eds., Ellis Horwood, London, 1984, p.653.

54. C. Rollins, L. Iensen and A. Schwarts, Anal. Chem., 34, 711 (1962).

55. N.H. Sweed and R.A. Gregory, AIChE., 17(1), 171 (1971).

56. R.H. Wilhelm, A.W. Rice, R.W. Rolke and N.H. Sweed, Ind. Eng. Chem. Fundam., 7(3), 337 (1968).

57. R.W. Rolke and R.H. Wilhelm, Ind. Eng. Chem. Fundam., 8(2), 235 (1969).

58. G. Simon, L. Hanak, G. Grevillot, T. Szanya and G. Marton, J. Chromatogr. B, 664, 17 (1995).

59. P.C. Wankat, Chem.Eng.Sci., 33, 723 (1976).

60. N.A.Tikhonov, Zh.Fiz.Khim., 68(5), 856 (1994) (Russian).

61. A.D. Poezd and N.A. Tikhonov, Zh.Fiz.Khim., 69 (3), 496 (1995) (Russian).

62. K. Cohen, Theory of Isotope Separation as Applied to the Large Scale Production of U-235, McGraw-Hill, New York (1951).

63. R.Kh. Khamizov, D.N. Muraviev and A. Warshawsky, in Ion Exchange and Solvent Extraction, Vol.12, J.B.Marinsky and Yi. Marcus, Eds., Marcel Dekker Inc., New-York - Basel - Hong-Kong, 1995, Ch. 2.

64. A.M. Rozen, Dokl.Acad.Nauk SSSR., 108 (1), 122 (1956) (Russian).

65. A.M. Rosen, Theory of Isotope Separation in Columns, Atomizdat, Moscow (1960) (Russian).

66. K. Bier, Chem.-Ing.-Techn., 28, 625 (1956).

67. K. Bier, Chem.-Ing.-Techn., 31 (1), 22 (1958).

68. G. Weiss, Chem.-Ing.-Techn., 30 (7), 433 (1958).

69. Ja.M. Warshavsky and S.E. Vaizberg, Khim. Nauka i Prom., 4(4), 498 (1959) (Russian).

70. N.M. Zhavoronkov and K.I. Sakodinskii, Usp. Khim., 29(9), 1112 (1960) (Russian).

71. B.M. Andreev, Ja.D. Zelvensky and S.G. Katal'nikov, Separation of Stable Isotopes by Physico-Chemical Methods, Energoatomizdat, Moscow (1982) (Russian).

72. B.M. Andreev, Ja.D. Zelvenskii and S.G. Katal'nikov, Heavy Hydrogen Isotopes in Nuclear Engineering, Energoatomizdat, Moscow, (1987) (Russian).

73. B.M. Andreev, Khim. Prom., 8, 581 (1962) (Russian).

74. M.S. Safonov and R.G. Iksanov, Teor. Osnovy Khim. Tekhnol. 7, 770 (1973) (Russian).

75. V.I. Gorshkov. A.M. Kurbanov and N.V. Apolonnik, Method for Separation of Substance Mixtures, Pat.USSR 373012 (1970).

76. V.I. Gorshkov, A.M. Kurbanov and M.V. Ivanova, Zh. Fiz. Khim., 49, 1276 (1975) (Russian).

77. V.I. Gorshkov, I.A. Kuznetsov, G.M. Panchenkov and L.V. Kustova, Zh. Neorg. Khim., 8, 2790 (1963) (Russian).

78. V.I. Gorshkov, M.S. Safonov and N.M. Voskresenskii, Ion Exchange in Counter-Current Columns, Nauka, Moscow (1981) (Russian).

79. V.A. Ivanov and V.I. Gorshkov, Teor. Osnovy Khim. Technol., 17, 723 (1983) (Russian).

80. M.S. Safonov and S.A. Borisov, Teor. Osnovy Khim. Technol. 15, 676 (1981) (Russian).

81. M.S. Safonov, N.M. Voskresenskii and B.M. Andreev, Teor. Osnovy Khim. Technol. 15, 163 (1981) (Russian).

82. V.A. Ivanov and V.I. Gorshkov, Dep. VINITI USSR No.3350-79, Moscow 21.09.1979.

83. M.S. Safonov, Teor. Osnovy Khim. Technol. 4(6), 813 (1970) (Russian).

84. V.A. Ivanov and V.I. Gorshkov, Zh. Fiz. Khim. 53(8), 2114 (1979) (Russian).

85. M.S. Safonov and R.G. Iksanov, Zh. Fiz. Khim. 48(2), 416 (1974) (Russian).

86. S.A. Borisov and M.S. Safonov, Teor. Osnovy Khim. Technol. 18(2), 159 (1984) (Russian).

87. M.S. Safonov and V.I. Gorshkov, Zh. Fiz. Khim., 42, 1992 (1968) (Russian).

88. M.V. Obrezkova, Ion exchange separation based on dependence of selectivity and sorption capacity of bi-functional ion exchanger on solution pH, Ph.D. Thesis, Moscow State University, Moscow, 1978.

89. V.A. Ivanov, Separation of mixtures of alkali metal ions in columns on bi-functional cation exchanger by combined scheme, Ph.D. Thesis, Moscow State University, Moscow, 1980.

90. V.A. Ivanov a32nd V.I. Gorshkov, Visokochistye Veschestva. 1(5), 100 (1987).

91. I.R. Higgins, Ind. Eng. Chem., 53(8), 635 (1961).

92. V.A. Ivanov, Ya.N. Malikh, V.I. Gorshkov and V.K. Belnov, Teor. Osnovy Khim. Technol. 22, 687 (1988) (Russian).

93. V.I. Gorshkov, in Ion Exchange and Solvent Extraction, V.12, J. Marinsky and Y. Marcus, Eds., Marcel Dekker, New-York, 1995, Ch. 2.